

# Accepted Manuscript

Organoantimony(III) halide complexes with azastibocine framework as potential antitumor agents: Correlation between cytotoxic activity and N→Sb inter-coordination

Jian Lei, Yongping Liu, Yingcan Ou, Chak-Tong Au, Yi Chen, Shuang-Feng Yin



PII: S0223-5234(19)30464-7

DOI: <https://doi.org/10.1016/j.ejmech.2019.05.054>

Reference: EJMECH 11364

To appear in: *European Journal of Medicinal Chemistry*

Received Date: 11 March 2019

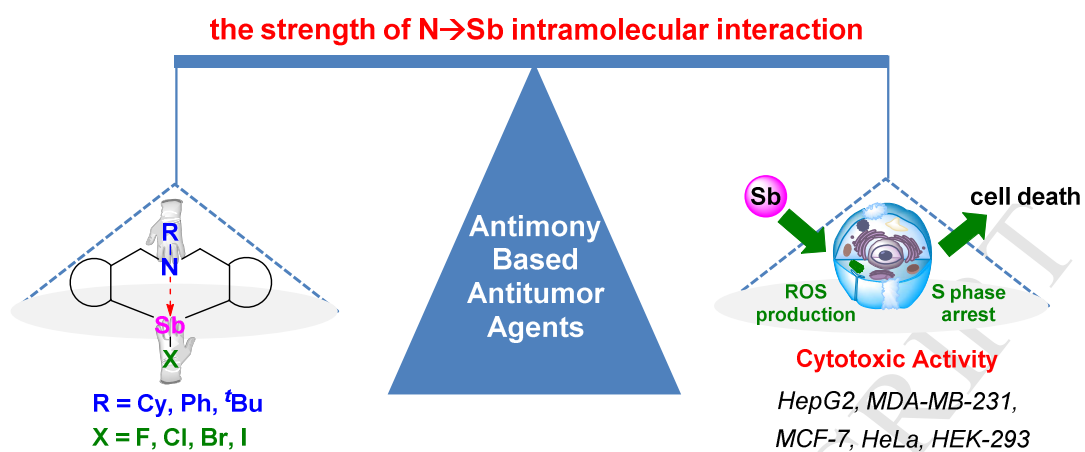
Revised Date: 2 May 2019

Accepted Date: 19 May 2019

Please cite this article as: J. Lei, Y. Liu, Y. Ou, C.-T. Au, Y. Chen, S.-F. Yin, Organoantimony(III) halide complexes with azastibocine framework as potential antitumor agents: Correlation between cytotoxic activity and N→Sb inter-coordination, *European Journal of Medicinal Chemistry* (2019), doi: <https://doi.org/10.1016/j.ejmech.2019.05.054>.

This is a PDF file of an unedited manuscript that has been accepted for publication. As a service to our customers we are providing this early version of the manuscript. The manuscript will undergo copyediting, typesetting, and review of the resulting proof before it is published in its final form. Please note that during the production process errors may be discovered which could affect the content, and all legal disclaimers that apply to the journal pertain.

## Graphic abstract



1 **Organoantimony(III) Halide Complexes with Azastibocine**  
2 **Framework as Potential Antitumor Agents: Correlation between**  
3 **Cytotoxic Activity and N→Sb Inter-Coordination**

4 Jian Lei <sup>a,b,1</sup>, Yongping Liu <sup>a,1</sup>, Yingcan Ou <sup>a</sup>, Chak-Tong Au <sup>c</sup>, Yi Chen <sup>a,b,\*</sup>,

5 Shuang-Feng Yin <sup>b,\*\*</sup>

6 <sup>a</sup> School of Medicine, Hunan University of Chinese Medicine, Changsha 410208, PR  
7 China

8 <sup>b</sup> State Key Laboratory of Chemo/Biosensing and Chemometrics, College of  
9 Chemistry and Chemical Engineering, Hunan University, Changsha 410082, PR  
10 China

11 <sup>c</sup> College of Chemistry and Chemical Engineering, Hunan Institute of Engineering,  
12 Xiangtan, 411104, PR China

13 \* Corresponding author. E-mail address: cscy1975@163.com (Y. Chen).

14 \*\* Corresponding author. E-mail address: sf\_yin@hnu.edu.cn (S.-F. Yin).

15 <sup>1</sup> Lei and Liu contributed equally to this work.

16 **Abstract**

17 The relationship between chemical structure and *in vitro* cytotoxic activities of a  
18 series of azastibocine-framework organoantimony(III) halide complexes against  
19 cancerous (HepG2, MDA-MB-231, MCF-7 and HeLa) and nonmalignant (HEK-293)  
20 cell lines was studied for the first time. A positive correlation between cytotoxic  
21 activity and the length of N→Sb coordinate bond on azastibocine framework of same  
22 nitrogen substituent was observed. By comparison, the organoantimony(III) complex  
23 6-cyclohexyl-12-fluoro-5,6,7,12-tetrahydrodibenzo[*c,f*][1,5]azastibocine (**C4**)  
24 exhibited the highest selectivity index, giving a IC<sub>50</sub>(nonmalignant)/IC<sub>50</sub>(cancerous)  
25 ratio of up to 8.33. The results of cell cycle analysis indicated that the inhibitory effect  
26 of **C4** on the cellular viability was caused by cell cycle arrest mainly at the S phase.  
27 The necrosis induced by **C4** was confirmed by the Trypan blue dye exclusion test and  
28 the increase of lactic dehydrogenase (LDH) released in the culture medium.  
29 Furthermore, evaluation of the levels of intracellular reactive oxygen species (ROS) in  
30 MDA-MB-231 cells, by quantifying the relative fluorescence units (RFU) using  
31 spectrofluorometer, indicated that cytotoxic activity of **C4** is dependent on the  
32 production of ROS. This work established the correlation between cytotoxic activity  
33 and N→Sb inter-coordination, a finding that provided theoretical and experimental  
34 basis for in-depth design of antimony-based organometallic complexes as potential  
35 anticancer agents.

36 **Keywords**

37 Organoantimony(III) complex; Cytotoxic Activity; Structure-activity relationship;  
38 Necrosis; Reactive oxygen species

39 **Abbreviations**

40 CCK-8, Cell Counting Kit-8; IC<sub>50</sub>, half-maximal inhibitory concentration; SI,  
41 selectivity index; PI, propidium iodide; PS, phosphatidylserine; LDH, lactic  
42 dehydrogenase; ROS, reactive oxygen species; DCFH-DA,  
43 5-(and-6)-carboxy-2',7'-dichlorodihydrofluorescein diacetate; NAC, *N*-acetylcysteine

## 44 **1. Introduction**

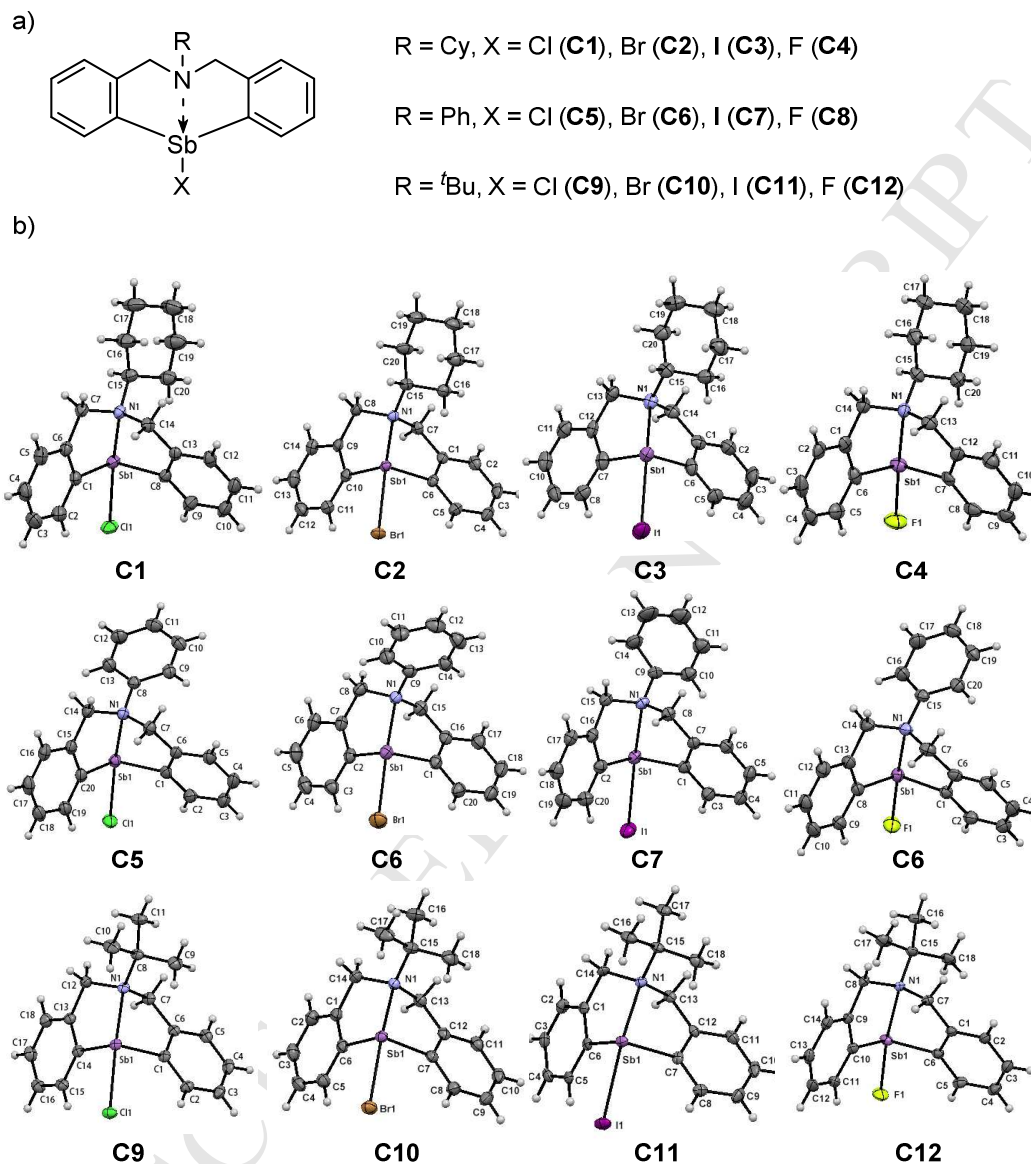
45 The rich diversity of coordination chemistry provides exciting prospects for the  
46 design of novel metallodrugs with unique biological activity [1]. Since the landmark  
47 report of cisplatin compounds in cancer therapy, continuous efforts have been made in  
48 the investigation of new metallic and organometallic complexes for the purpose of  
49 developing metal-based chemotherapeutics of low toxicity that are endowed with  
50 anticancer activity [2–6].

51 In the past century, antimony-based drugs have been extensively investigated  
52 because of their clinically therapeutic efficacy against leishmaniosis [7,8]. Like  
53 cancer, the parasite divides rapidly and may share some common pathways that could  
54 be targets for chemotherapy [7,8]. Therefore, there is an increasing interest in  
55 antitumor application of antimony compounds, and significant progress has been  
56 made [9,10]. For instance, inorganic trivalent antimonials such as  $\text{Sb}_2\text{O}_3$  were found  
57 to show biological effects on acute promyelocytic leukemia (APL) that closely  
58 resemble those of  $\text{As}_2\text{O}_3$  [11]. A number of antimony(III) compounds complexed with  
59 polydentate ligands such as carboxylic acids [12–14], hydrazones [15], thioamides  
60 [16], and dithiocarbamates [17], were synthesized and assessed as biomedical agents  
61 for anticancer purpose. Currently, the most studied antimony(III) compounds in the  
62 context of antitumor activity are the ones with at least one antimony–carbon covalent  
63 bond, the so-called organoantimony complexes [18–24]. The first example showing  
64 the antitumor property of organoantimony(III) species was reported by Silvestru and  
65 coworkers, wherein they found that diphenylantimony(III) derivatives of

66 dithiophosphorus ligands exhibited inhibitory effects on the growth of Ehrlich ascites  
67 tumor [18]. Meanwhile, the pharmacological applications of antimony(V)-based  
68 organometallic complexes in cancerous cells proliferation were also reported [25–29].  
69 The potential inhibitory effects of triphenylantimony(V) polyamines on cancer-related  
70 cell lines were described by Carraher *et al.* [25]. Demicheli and coworkers disclosed  
71 the *in vitro* cytotoxic activity of a series of pentavalent organoantimony complexes  
72 against malignant carcinoma cells, such as human chronic myelogenous leukemia  
73 (K562) and murine metastatic melanoma (B16F10) [26,27]. Arylantimony(V)  
74 derivatives of *exo*-7-oxa-bicyclo[2,2,1]heptane (ene)-3-arylamide-2-acid and  
75 arylhydroxamic acid were introduced by Li and coworkers as potential antitumor  
76 agents against a diversity of human neoplastic cell lines [27,28]. Among those  
77 antimony-based metallic and organometallic complexes, the presence of coordination  
78 between antimony center and ligand is relevant to their cellular activity. In most cases,  
79 the coordination of antimony by ligands resulted in compounds with antitumor  
80 potency greater than that of the uncoordinated ligands [13,15,27–29] as well as their  
81 antimony-containing precursors [15,28,29]. The strong development in this field  
82 motivated us to elucidate the relationship between coordination effect and antitumor  
83 potency for the purpose of developing organoantimony-based chemotherapeutics in  
84 cancer therapy. To our knowledge, relatively few information is available in the  
85 literature about the related chemistry between coordination effect and antitumor  
86 activity of antimony-based organometallic complexes.

87 Previously our group reported the anti-proliferative activity of heterocyclic

88 hypervalent organoantimony(III) complexes on human alveolar adenocarcinoma cell  
89 line (A549) [30]. Although full details are yet to be revealed, preliminary data have  
90 indicated that anti-proliferative activity detected over these complexes could be  
91 attributed to the coordination between the antimony and nitrogen atoms. Very  
92 recently, Hadjikakou and coworkers developed a series of antimony(III) halide  
93 complexes with dithiocarbamate ligands, and they found that the halogen type causes  
94 no influence on the antitumor activity [17]. With this in mind, we herein revealed for  
95 the first time the correlation between cytotoxicity and coordination effect by studying  
96 the *in vitro* structure-activity relationship (SAR) of a series of azastibocine-framework  
97 organoantimony(III) halide complexes against different cell lines, including solid  
98 cancerous (human liver hepatocellular carcinoma cell line, HepG2; human breast  
99 cancer cell line, MDA-MB-231; human breast adenocarcinoma cell line, MCF-7; and  
100 human cervical carcinoma cell line HeLa) and nonmalignant (human embryonic  
101 kidney cell line, HEK-293) cells. Moreover, considering the selectivity index that is  
102 derived from  $IC_{50}(\text{nonmalignant})/IC_{50}(\text{cancerous})$  ratio, the most potent compound **C4**  
103 was selected for further mechanistic investigation. Finally, we describe  
104 organoantimony complex **C4** driven induction of necrosis in MDA-MB-231 cells  
105 through intracellular ROS production.

106 **2 Results and Discussion**107 **2.1 Chemistry**

108

109 **Fig.1.** a) Molecular structures of organoantimony(III) halide complexes with azastibocine

110 framework. b) ORTEP diagram of the X-ray molecular structure of organoantimony(III)

111 complexes **C1–C12**.

**Table 1**

Selected bond lengths (Å) and angles (deg) of organoantimony(III) halide complexes **C1**–**C12**.

| <b>C1</b>        |           | <b>C2</b>        |           | <b>C3</b>       |           | <b>C4</b>        |           |
|------------------|-----------|------------------|-----------|-----------------|-----------|------------------|-----------|
| Sb(1)-C(1)       | 2.144(4)  | Sb(1)-C(6)       | 2.143(2)  | Sb(1)-C(6)      | 2.154(3)  | Sb(1)-C(6)       | 2.140(3)  |
| Sb(1)-C(8)       | 2.134(4)  | Sb(1)-C(10)      | 2.157(2)  | Sb(1)-C(7)      | 2.166(3)  | Sb(1)-C(7)       | 2.145(3)  |
| C(1)-Sb(1)-C(8)  | 98.2(1)   | C(6)-Sb(1)-C(10) | 99.23(8)  | C(6)-Sb(1)-C(7) | 98.8(1)   | C(6)-Sb(1)-C(7)  | 98.5(1)   |
| Cl(1)-Sb(1)-N(1) | 162.92(7) | Br(1)-Sb(1)-N(1) | 163.53(4) | I(1)-Sb(1)-N(1) | 163.34(6) | F(1)-Sb(1)-N(1)  | 156.42(7) |
| Sb(1)-N(1)       | 2.397(2)  | Sb(1)-N(1)       | 2.387(2)  | Sb(1)-N(1)      | 2.400(2)  | Sb(1)-N(1)       | 2.450(2)  |
| Sb(1)-Cl(1)      | 2.5572(9) | Sb(1)-Br(1)      | 2.7142(5) | Sb(1)-I(1)      | 2.9650(4) | Sb(1)-F(1)       | 2.015(2)  |
| <b>C5</b>        |           | <b>C6</b>        |           | <b>C7</b>       |           | <b>C8</b>        |           |
| Sb(1)-C(1)       | 2.150(2)  | Sb(1)-C(1)       | 2.158(3)  | Sb(1)-C(1)      | 2.166(3)  | Sb(1)-C(1)       | 2.131(3)  |
| Sb(1)-C(8)       | 2.155(2)  | Sb(1)-C(8)       | 2.156(3)  | Sb(1)-C(8)      | 2.175(3)  | Sb(1)-C(8)       | 2.153(3)  |
| C(1)-Sb(1)-C(8)  | 100.53(7) | C(1)-Sb(1)-C(8)  | 100.4(1)  | C(1)-Sb(1)-C(8) | 96.3(1)   | C(1)-Sb(1)-C(8)  | 91.80(9)  |
| Cl(1)-Sb(1)-N(1) | 161.98(4) | Br(1)-Sb(1)-N(1) | 163.22(6) | I(1)-Sb(1)-N(1) | 163.92(6) | F(1)-Sb(1)-N(1)  | 162.92(7) |
| Sb(1)-N(1)       | 2.466(2)  | Sb(1)-N(1)       | 2.469(2)  | Sb(1)-N(1)      | 2.498(3)  | Sb(1)-N(1)       | 2.522(2)  |
| Sb(1)-Cl(1)      | 2.5173(5) | Sb(1)-Br(1)      | 2.6620(4) | Sb(1)-I(1)      | 2.8995(3) | Sb(1)-F(1)       | 1.998(2)  |
| <b>C9</b>        |           | <b>C10</b>       |           | <b>C11</b>      |           | <b>C12</b>       |           |
| Sb(1)-C(1)       | 2.147(2)  | Sb(1)-C(6)       | 2.153(2)  | Sb(1)-C(6)      | 2.166(3)  | Sb(1)-C(6)       | 2.127(7)  |
| Sb(1)-C(14)      | 2.155(3)  | Sb(1)-C(7)       | 2.151(2)  | Sb(1)-C(7)      | 2.157(3)  | Sb(1)-C(10)      | 2.135(7)  |
| C(1)-Sb(1)-C(14) | 95.60(9)  | C(6)-Sb(1)-C(7)  | 96.18(8)  | C(6)-Sb(1)-C(7) | 97.6(1)   | C(6)-Sb(1)-C(10) | 98.2(3)   |
| Cl(1)-Sb(1)-N(1) | 161.60(5) | Br(1)-Sb(1)-N(1) | 162.99(4) | I(1)-Sb(1)-N(1) | 163.59(6) | F(1)-Sb(1)-N(1)  | 155.9(2)  |
| Sb(1)-N(1)       | 2.467(2)  | Sb(1)-N(1)       | 2.446(2)  | Sb(1)-N(1)      | 2.462(3)  | Sb(1)-N(1)       | 2.495(5)  |
| Sb(1)-Cl(1)      | 2.5579(7) | Sb(1)-Br(1)      | 2.7631(5) | Sb(1)-I(1)      | 2.9463(3) | Sb(1)-F(1)       | 2.026(6)  |

112 The synthesis of organoantimony chlorides, which were labeled **C1**, **C5** and **C9**,  
 113 was carried out as previously reported [30]. Organoantimony bromides, iodides, and  
 114 fluorides could be prepared by mixing the organoantimony chlorides with the  
 115 corresponding inorganic salts (i.e. potassium bromide, potassium iodide or silver  
 116 fluoride) in 1:10 or 1:1 molar ratio as specified in the Experimental Section. Fig. 1a  
 117 depicts the general molecular structures of the complexes of formula  
 118  $\text{RN}(\text{CH}_2\text{C}_6\text{H}_4)\text{SbX}$ , where R = Cy (cyclohexyl), Ph (phenyl), or <sup>t</sup>Bu (tertiary butyl)  
 119 and X = Cl, Br, I, F. These complexes readily recrystallized from the reaction  
 120 mixtures as colorless crystals in moderate to excellent yields and could be kept in  
 121 open air for a long-term period without showing any detectable change in <sup>1</sup>H NMR

122 spectra (see Supplementary Materials for details).

123 The molecular structures of **C1–C12** are unambiguously characterized by NMR  
124 spectroscopy, elemental analysis as well as single crystal X-ray diffraction analysis.  
125 The ORTEP diagrams of these complexes revealed that the central  
126 antimony-containing part shows analogous pseudo-trigonal bipyramidal structures  
127 with a butterfly-shaped ligand where the nitrogen and halogen atoms are located at the  
128 apical positions and the two carbon atoms adjacent to the antimony atom are at the  
129 equatorial positions along with a lone electron pair of antimony (Fig. 1b). The lengths  
130 of N→Sb coordinate bond in these complexes are within the 2.387(2)–2.522(2) Å  
131 range (Table 1), which are slightly longer than the sum of the covalent radii (2.11 Å)  
132 but much shorter than the sum of the van der Waals radii (3.74 Å) [31,32]. The results  
133 evidence the inter-coordination between the antimony and the nitrogen atoms, and the  
134 strength of N→Sb coordination on the azastibocine framework could be adjusted by  
135 synergistic modulating the property of nitrogen substituents and halogen atoms  
136 adjacent to the central antimony atom. The lengths of N→Sb coordinate bond of  
137 phenyl derivatives (**C5–C8**) are obviously longer than those of cyclohexyl derivatives  
138 (**C1–C4**). Given the inverse electronic properties of phenyl and cyclohexyl group, it is  
139 apparent that the strength of N→Sb inter-coordination is weakened with the increase  
140 of electron-withdrawing ability of the nitrogen substituents. The steric effect of the  
141 nitrogen substituents also significantly affect the intramolecular interaction between  
142 the antimony and nitrogen atoms, as seen in the lengths of N→Sb coordinate bond of  
143 *tert*-butyl derivatives **C9–C12**. In addition, the coordinate bond lengths of

144 organoantimony(III) fluorides [2.450(2) Å, **C4**; 2.522(2) Å, **C8**; 2.495(5) Å, **C12**] are  
 145 distinctly longer than those of chlorides, bromides and iodides, owing to the strong  
 146 electron-withdrawing ability of fluorine atom.

**Table 2**Crystallographic data for organoantimony(III) halide complexes **C1–C12**.

| Complex                             | <b>C1</b>                             | <b>C2</b>                             | <b>C3</b>                             | <b>C4</b>                             | <b>C5</b>                             | <b>C6</b>                             |
|-------------------------------------|---------------------------------------|---------------------------------------|---------------------------------------|---------------------------------------|---------------------------------------|---------------------------------------|
| Empirical formula                   | C <sub>20</sub> H <sub>23</sub> ClNSb | C <sub>20</sub> H <sub>23</sub> BrNSb | C <sub>20</sub> H <sub>23</sub> INSb  | C <sub>20</sub> H <sub>23</sub> FNSb  | C <sub>20</sub> H <sub>17</sub> ClNSb | C <sub>20</sub> H <sub>17</sub> BrNSb |
| Formula weight                      | 434.59                                | 479.05                                | 526.04                                | 418.14                                | 428.55                                | 473.01                                |
| Temperature/K                       | 293                                   | 273                                   | 100                                   | 100                                   | 273                                   | 298                                   |
| Crystal system                      | monoclinic                            | monoclinic                            | monoclinic                            | monoclinic                            | monoclinic                            | monoclinic                            |
| Space group                         | <i>P2(1)/c</i>                        | <i>P2(1)/n</i>                        | <i>P2(1)/n</i>                        | <i>P2(1)/n</i>                        | <i>P2(1)/n</i>                        | <i>P2(1)/n</i>                        |
| <i>a</i> /Å                         | 10.0771(7)                            | 10.2338(5)                            | 11.3664(3)                            | 9.3503(3)                             | 9.3782(4)                             | 9.5744(3)                             |
| <i>b</i> /Å                         | 16.2881(12)                           | 16.5885(7)                            | 12.5996(3)                            | 15.9263(5)                            | 10.1833(4)                            | 10.2962(3)                            |
| <i>c</i> /Å                         | 12.2040(9)                            | 12.0033(5)                            | 13.0792(4)                            | 11.7239(4)                            | 18.1033(8)                            | 18.1939(6)                            |
| $\alpha$ /°                         | 90.00                                 | 90.00                                 | 90.00                                 | 90.00                                 | 90.00                                 | 90.00                                 |
| $\beta$ /°                          | 111.812(10)                           | 113.346(2)                            | 94.703(2)                             | 104.044(3)                            | 102.895(10)                           | 100.795(1)                            |
| $\gamma$ /°                         | 90.00                                 | 90.00                                 | 90.00                                 | 90.00                                 | 90.00                                 | 90.00                                 |
| <i>V</i> /Å <sup>3</sup>            | 1859.7(2)                             | 1870.89(15)                           | 1866.79(9)                            | 1693.69(10)                           | 1685.3(12)                            | 1761.81(10)                           |
| <i>Z</i>                            | 4                                     | 4                                     | 4                                     | 4                                     | 4                                     | 4                                     |
| No. of reflections collected        | 10058                                 | 30234                                 | 12759                                 | 10827                                 | 9923                                  | 10613                                 |
| No. of unique reflections           | 3644                                  | 4636                                  | 3284                                  | 2982                                  | 4032                                  | 3417                                  |
| <i>R</i> <sub>int</sub>             | 0.047                                 | 0.0363                                | 0.0390                                | 0.0376                                | 0.015                                 | 0.038                                 |
| <i>R</i> <sub>1(reflections)</sub>  | 0.0324                                | 0.0196                                | 0.0236                                | 0.0256                                | 0.0203                                | 0.0294                                |
| <i>wR</i> <sub>2(reflections)</sub> | 0.0917                                | 0.0416                                | 0.0561                                | 0.0598                                | 0.0560                                | 0.0709                                |
| GOF on <i>F</i> <sup>2</sup>        | 1.048                                 | 1.066                                 | 1.022                                 | 1.097                                 | 1.077                                 | 1.041                                 |
| Complex                             | <b>C7</b>                             | <b>C8</b>                             | <b>C9</b>                             | <b>C10</b>                            | <b>C11</b>                            | <b>C12</b>                            |
| Empirical formula                   | C <sub>20</sub> H <sub>17</sub> INSb  | C <sub>20</sub> H <sub>17</sub> FNSb  | C <sub>18</sub> H <sub>21</sub> ClNSb | C <sub>18</sub> H <sub>21</sub> BrNSb | C <sub>18</sub> H <sub>21</sub> INSb  | C <sub>18</sub> H <sub>21</sub> FNSb  |
| Formula weight                      | 520.00                                | 412.10                                | 408.56                                | 453.02                                | 500.01                                | 392.11                                |
| Temperature/K                       | 298                                   | 293                                   | 273                                   | 273                                   | 100                                   | 273                                   |
| Crystal system                      | monoclinic                            | monoclinic                            | monoclinic                            | monoclinic                            | monoclinic                            | monoclinic                            |
| Space group                         | <i>P2(1)/c</i>                        | <i>P2(1)/n</i>                        | <i>P2(1)/n</i>                        | <i>P2(1)/n</i>                        | <i>P2(1)/c</i>                        | <i>Cc</i>                             |
| <i>a</i> /Å                         | 9.1637(3)                             | 10.2974(8)                            | 9.7692(12)                            | 9.8178(4)                             | 12.3974(4)                            | 17.7432(9)                            |
| <i>b</i> /Å                         | 10.9833(4)                            | 10.3031(8)                            | 15.933(2)                             | 16.1278(5)                            | 9.4136(3)                             | 10.6409(6)                            |
| <i>c</i> /Å                         | 18.0957(7)                            | 15.7161(11)                           | 11.4491(14)                           | 11.4078(5)                            | 14.8803(5)                            | 17.8551(10)                           |
| $\alpha$ /°                         | 90.00                                 | 90.00                                 | 90.00                                 | 90.00                                 | 90.00                                 | 90.00                                 |
| $\beta$ /°                          | 95.784(1)                             | 101.559(1)                            | 110.103(2)                            | 109.895(1)                            | 92.218(3)                             | 96.996(2)                             |
| $\gamma$ /°                         | 90.00                                 | 90.00                                 | 90.00                                 | 90.00                                 | 90.00                                 | 90.00                                 |
| <i>V</i> /Å <sup>3</sup>            | 1812.02(11)                           | 1633.6(2)                             | 1673.5(4)                             | 1698.50(11)                           | 1735.29(10)                           | 3346.0(3)                             |
| <i>Z</i>                            | 4                                     | 4                                     | 4                                     | 4                                     | 4                                     | 8                                     |
| No. of reflections collected        | 9043                                  | 9422                                  | 9317                                  | 49645                                 | 11089                                 | 31989                                 |
| No. of unique reflections           | 3510                                  | 3560                                  | 3889                                  | 2978                                  | 3058                                  | 8232                                  |
| <i>R</i> <sub>int</sub>             | 0.055                                 | 0.063                                 | 0.027                                 | 0.0437                                | 0.0353                                | 0.0229                                |
| <i>R</i> <sub>1(reflections)</sub>  | 0.0354                                | 0.0323                                | 0.0326                                | 0.0143                                | 0.0237                                | 0.0419                                |
| <i>wR</i> <sub>2(reflections)</sub> | 0.0912                                | 0.0840                                | 0.0860                                | 0.0541                                | 0.0516                                | 0.1205                                |
| GOF on <i>F</i> <sup>2</sup>        | 1.070                                 | 1.065                                 | 1.058                                 | 1.028                                 | 1.040                                 | 1.079                                 |

147 2.2 Biological activity

## 148 2.2.1 Anticancer/cytotoxic activity and structure-activity relationship (SAR) study

**Table 3**

Cytotoxic effect of organoantimony(III) halide complexes **C1–C12**, nitrogen-containing precursors **P1–P3** and cisplatin on various cancerous and nonmalignant cell lines after 24 h.

| Cell lines | HepG2                              |                 | MDA-MB-231            |                 | MCF-7                 |                 | HeLa                  |                 | HEK-293               |
|------------|------------------------------------|-----------------|-----------------------|-----------------|-----------------------|-----------------|-----------------------|-----------------|-----------------------|
| Compound   | IC <sub>50</sub> ± SD <sup>a</sup> | SI <sup>b</sup> | IC <sub>50</sub> ± SD | SI <sup>c</sup> | IC <sub>50</sub> ± SD | SI <sup>d</sup> | IC <sub>50</sub> ± SD | SI <sup>e</sup> | IC <sub>50</sub> ± SD |
| <b>C1</b>  | 1.84 ± 0.42                        | 5.05            | 1.40 ± 0.32           | 6.64            | 6.08 ± 1.38           | 1.53            | 1.63 ± 0.49           | 5.70            | 9.29 ± 1.16           |
| <b>C2</b>  | 4.86 ± 0.91                        | 2.10            | 3.63 ± 0.87           | 2.82            | 6.39 ± 1.45           | 1.60            | 3.12 ± 0.45           | 3.28            | 10.23 ± 0.55          |
| <b>C3</b>  | 1.61 ± 0.33                        | 5.63            | 1.28 ± 0.54           | 7.08            | 5.79 ± 1.56           | 1.56            | 1.13 ± 0.21           | 8.02            | 9.06 ± 1.31           |
| <b>C4</b>  | 1.06 ± 0.17                        | 7.15            | 0.91 ± 0.22           | 8.33            | 2.14 ± 0.93           | 3.54            | 0.93 ± 0.15           | 8.15            | 7.58 ± 0.89           |
| <b>C5</b>  | 2.78 ± 0.59                        | 3.07            | 1.72 ± 0.33           | 4.97            | 3.14 ± 0.81           | 2.72            | 3.32 ± 0.50           | 2.57            | 8.54 ± 1.88           |
| <b>C6</b>  | 1.90 ± 0.12                        | 4.10            | 1.05 ± 0.13           | 7.42            | 2.61 ± 0.60           | 2.98            | 2.34 ± 0.32           | 3.33            | 7.79 ± 1.36           |
| <b>C7</b>  | 1.87 ± 0.11                        | 3.33            | 1.04 ± 0.11           | 5.98            | 2.39 ± 1.67           | 2.60            | 2.06 ± 0.29           | 3.02            | 6.22 ± 1.69           |
| <b>C8</b>  | 0.88 ± 0.32                        | 4.41            | 0.52 ± 0.02           | 7.46            | 2.31 ± 0.32           | 1.68            | 1.12 ± 0.21           | 3.46            | 3.88 ± 1.01           |
| <b>C9</b>  | 1.41 ± 0.06                        | 4.03            | 0.84 ± 0.23           | 6.76            | 3.41 ± 0.30           | 1.67            | 1.98 ± 0.54           | 2.87            | 5.68 ± 1.32           |
| <b>C10</b> | 2.74 ± 0.63                        | 2.27            | 1.85 ± 0.25           | 3.36            | 6.34 ± 1.31           | 0.98            | 4.78 ± 0.83           | 1.30            | 6.22 ± 1.07           |
| <b>C11</b> | 1.84 ± 0.28                        | 4.05            | 0.97 ± 0.19           | 7.69            | 4.89 ± 1.13           | 1.53            | 2.09 ± 0.62           | 3.57            | 7.46 ± 0.66           |
| <b>C12</b> | 0.71 ± 0.06                        | 3.51            | 0.51 ± 0.12           | 4.88            | 0.96 ± 0.83           | 2.59            | 1.08 ± 0.47           | 2.31            | 2.49 ± 0.67           |
| <b>P1</b>  | >50.00                             | -               | >50.00                | -               | >50.00                | -               | >50.00                | -               | >50.00                |
| <b>P2</b>  | >50.00                             | -               | >50.00                | -               | >50.00                | -               | >50.00                | -               | >50.00                |
| <b>P3</b>  | >50.00                             | -               | >50.00                | -               | >50.00                | -               | >50.00                | -               | >50.00                |
| cisplatin  | 13.19 ± 4.51                       | 3.71            | 12.63 ± 1.22          | 3.88            | 22.75 ± 8.59          | 2.15            | 17.35 ± 3.64          | 2.82            | 48.96 ± 8.75          |

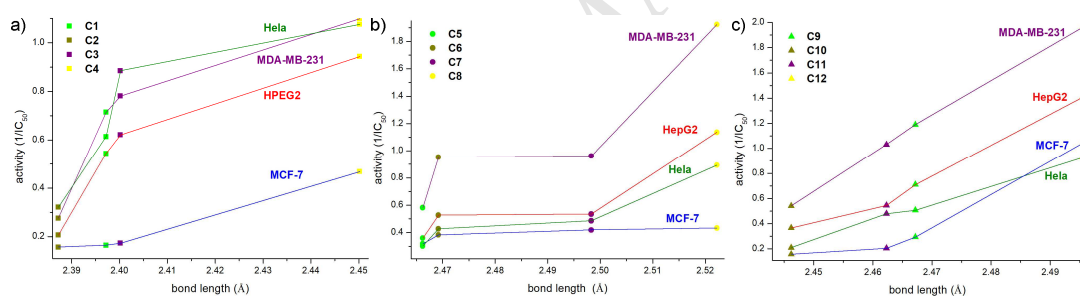
Cancerous Cell Lines: HepG2 (human liver hepatocellular carcinoma cell line), MDA-MB-231 (human breast cancer cell line), MCF-7 (human breast adenocarcinoma cell line) and HeLa (human cervical carcinoma cell line). Nonmalignant Cell Line: HEK-293 (human embryonic kidney cell line). IC<sub>50</sub>: concentration that is cytotoxic against 50% of cell lines. SI: selectivity index. <sup>a</sup> The IC<sub>50</sub> values were determined through non-linear regression analysis; Each well was triplicated and each experiment was repeated at least three times. IC<sub>50</sub> values quoted are mean ± SD (μM). <sup>b</sup> Calculated as the ratio between IC<sub>50</sub> in HEK-293 cells and IC<sub>50</sub> in HepG2. <sup>c</sup> Calculated as the ratio between IC<sub>50</sub> in HEK-293 cells and IC<sub>50</sub> in MDA-MB-231. <sup>d</sup> Calculated as the ratio between IC<sub>50</sub> in HEK-293 cells and IC<sub>50</sub> in MCF-7. <sup>e</sup> Calculated as the ratio between IC<sub>50</sub> in HEK-293 cells and IC<sub>50</sub> in HeLa.

149 The anticancer activity of the synthesized organoantimoy(III) halide complexes was  
 150 evaluated in a panel of four human solid tumor cell lines derived from hepatocellular  
 151 carcinoma (HepG2), breast cancer (MDA-MB-231 and MCF-7) and cervical  
 152 carcinoma (HeLa), together with cisplatin as positive control. Cell viability was  
 153 assessed using Cell Counting Kit-8 (CCK-8) as described and the results of  
 154 half-maximal inhibitory concentration (IC<sub>50</sub>) that represents the drug concentration  
 155 required to inhibit cell growth by 50% are summarized in Table 3. The results

156 demonstrated that all of the organoantimony(III) halide complexes exhibited much  
157 higher cytotoxic activity against the selected cancerous cell lines than cisplatin and  
158 the nitrogen-containing precursors **P1–P3**. It was also observed that the modulation of  
159 the type of the nitrogen substituent and halogen atom on the  
160 tetrahydrodibenzo[*c,f*][1,5]azastibocine framework would result in distinct  
161 antineoplastic performance towards the same cancerous cell line.

162 To further elucidate the related chemistry between coordination effect and  
163 cytotoxic activity of organoantimony complexes, a systematic structure-activity  
164 relationship study was explored. Given the different electronic and steric properties of  
165 the nitrogen substituents as well as based on the results of our preliminary study on  
166 antimony-based organometallic antitumor agents [30], a ranking of cytotoxic activity  
167 across the organoantimony complexes with the same nitrogen substituent (e.g.  
168 cyclohexyl, phenyl and tertiary butyl) and N→Sb coordinate bond length was  
169 performed (Fig. 2a–c). In each case, the nonlinear correlations between the lengths of  
170 N→Sb coordinate bond, which were modulated simply by the halogen type, and the  
171 cytotoxic activities of the corresponding organoantimony halide complexes were  
172 found, respectively. When the complexes were ranked by decreasing coordination  
173 effect, i.e., with increasing N→Sb coordinate bond lengths, the complexes having the  
174 same nitrogen substituent showed increasing inhibitory activities on all four cancerous  
175 cell lines. On the other hand, the most potent cytotoxic activities were observed over  
176 the organoantimony fluorides (**C4**, **C8** and **C12**) in each set, albeit there is no trend  
177 for the complexes bearing the other halogens (e.g. chloride, bromide and iodide).

178 According to this relationship and experimental results, we deduce that the cytotoxic  
 179 activity of these complexes was determined by the level of exposure of the  
 180 antimony(III) center. With decreasing extent of N→Sb coordination, the cytotoxic  
 181 activities of organometal moiety towards cancerous cells were increased. In other  
 182 words, the nitrogen-containing ligand may serve as an auxiliary moiety to decrease  
 183 the cytotoxicity of the antimony(III) center. With this in mind, we speculate that there  
 184 are two potential functions of N→Sb inter-coordination in these organoantimony(III)  
 185 complexes: (1) maintaining the skeleton structure to improve the air-stability and  
 186 water-tolerance; (2) reducing the level of exposure of the antimony(III) center to  
 187 decrease the cytotoxicity of trivalent antimonial.



188  
 189 **Fig. 2.** Correlation between N→Sb coordinate bond length in organoantimony complexes  
 190 with the same nitrogen substituent (a: cyclohexyl; b: phenyl; c: *tert*-butyl) and corresponding  
 191 anticancer activity against human tumor cells: HepG2 (red line), MDA-MB-231 (purple line),  
 192 MCF-7 (blue line) and HeLa (green line).

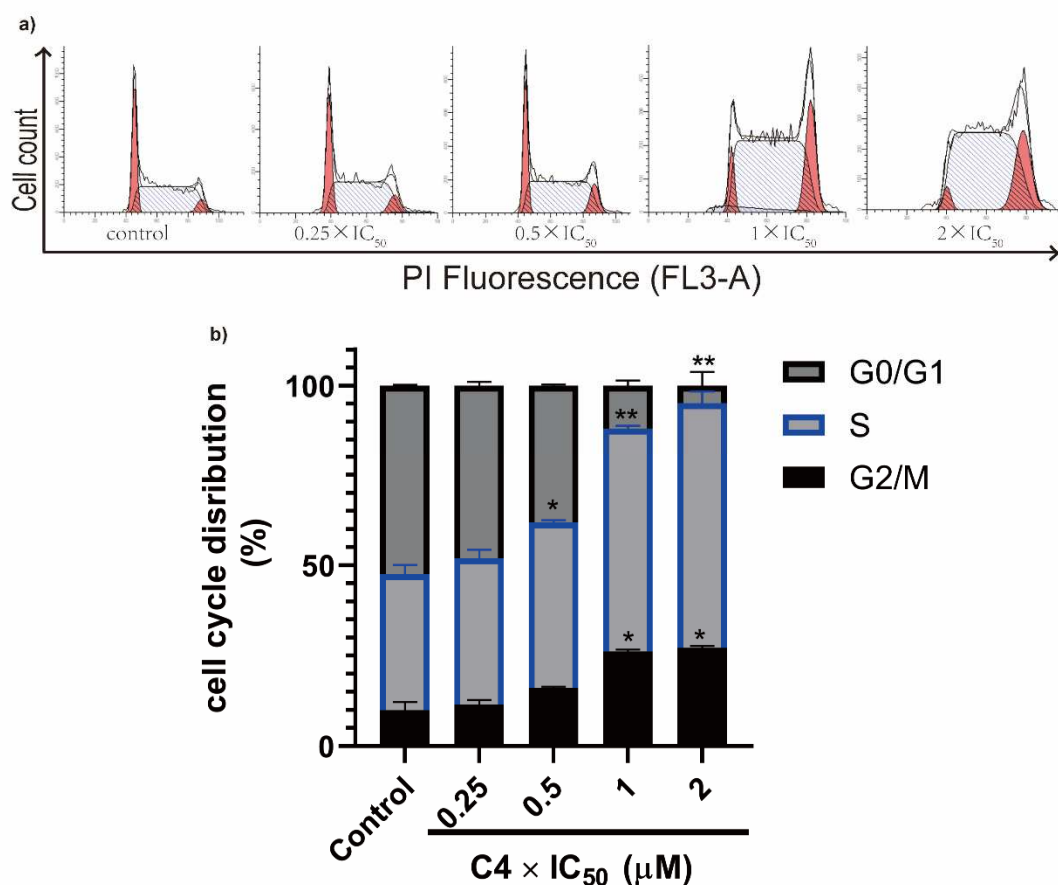
193 To test the effect of these organoantimony(III) halide complexes on nonmalignant  
 194 cells, we employed human embryonic kidney cells (HEK-293). The study of the  
 195 effects of these twelve complexes on nonmalignant cells is of particular interest in  
 196 terms of their potential application in clinical practice. After 24 h incubation, the IC<sub>50</sub>  
 197 values of complexes **C1–C12** on HEK-293 are within the 2.49–10.23 μM range. By

198 comparison with the commercial cisplatin, the majority of the synthesized  
199 organoantimony(III) complexes exhibited relatively higher selectivity index in the  
200 biological tests, especially so with the complex **C4**  
201 6-cyclohexyl-12-fluoro-5,6,7,12-tetrahydrodibenzo[*c,f*][1,5]azastibocine, which gives  
202 a  $IC_{50}(\text{nonmalignant})/IC_{50}(\text{cancerous})$  ratio of up to 8.33. With such a performance,  
203 **C4** opens a potential therapeutic window for antimony-based organometallic  
204 antitumor drugs, and we focused our investigation on the mechanistic study of **C4** in  
205 MDA-MB-231 cells.

#### 206 2.2.2 Cell Cycle Analysis

207 Generally, metal-based chemotherapeutic agents exhibit perturbation effect on cell  
208 cycle that is composed of  $G_1$ , S,  $G_2$ , M, and  $G_0$  phases in proliferating cells [33,34].  
209 At different stages of the cell cycle, cell nuclei contain different amounts of DNA.  
210 Therefore, according to the DNA content detected by propidium iodide (PI) staining,  
211 cell cycle is commonly described on the basis of  $G_0/G_1$ , S, and  $G_2/M$  phases. To  
212 investigate whether the cytotoxic effect of **C4** was caused by cell cycle arrest, PI  
213 staining and flow cytometry analysis of cells was performed in MDA-MB-231 cells.  
214 As shown in Fig. 3, after independently incubated with **C4** at 0.25, 0.5, 1, and 2  
215 equipotent concentrations of  $IC_{50}$  (0.91  $\mu\text{M}$ ) for 24 h, the MDA-MB-231 cells in  
216  $G_0/G_1$  phase showed a significant population decrease from 50.4% (untreated cells) to  
217 3.7% (1.82  $\mu\text{M}$  of **C4**), accompanied by a dose-dependent increase in the fraction of  
218 cells in the S (68.9% compare to 39.8% in untreated cells) and  $G_2/M$  phases (26.8%  
219 *versus* 9.8%). The results confirmed the retardation effect of organoantimony fluoride

220 C4 on the cell cycle progression, and it is reasonable to deduce that the observed  
 221 inhibitory effect on the cellular viability of MDA-MB-231 cells was caused by cell  
 222 cycle arrest mainly at the S phase, which represents a period of DNA replication.

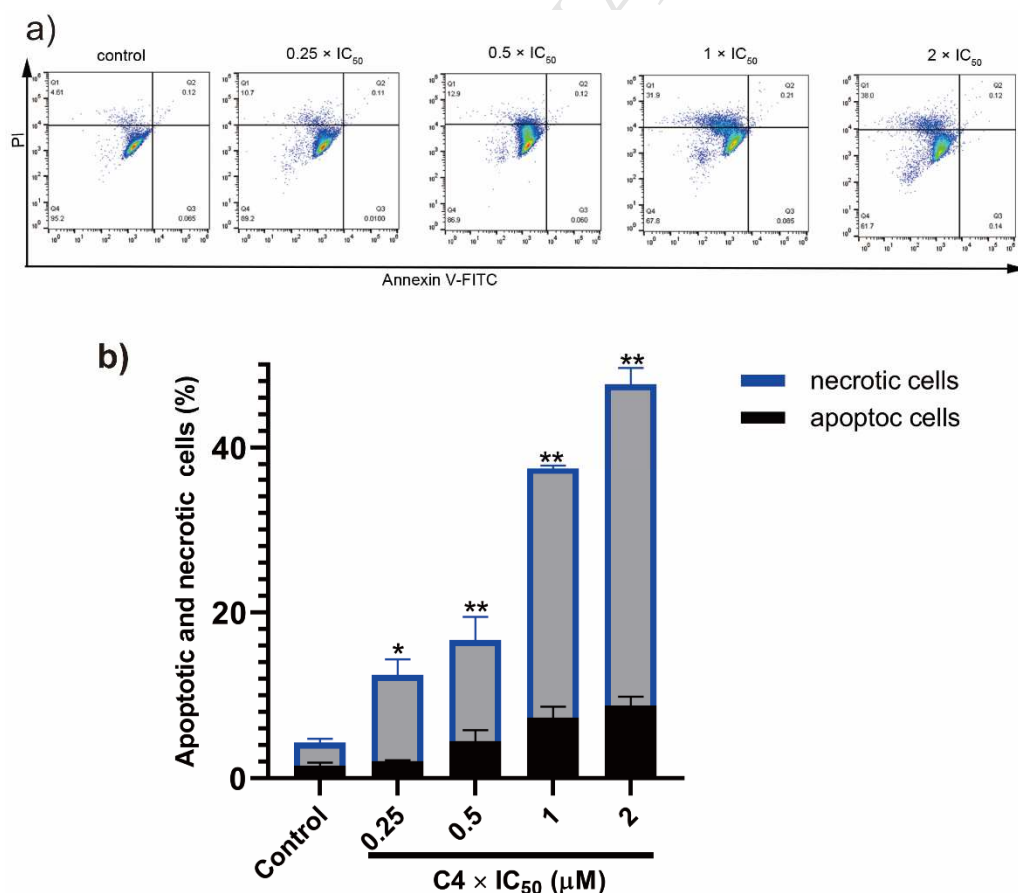


223  
 224 **Fig. 3.** Effect of C4 on the cell cycle distribution of MDA-MB-231 cells. a) Flow cytometry  
 225 analysis was performed on MDA-MB-231 cells treated with C4 for 24 h. b) With the  
 226 percentages of cells in different phases quantified. Data were shown as mean ± S.D. (n=3). \**P*  
 227 < 0.05, \*\**P* < 0.01 compared with the population of cells in the control group.

### 228 2.2.3 Apoptosis assay

229 Because prolonged cell cycle arrest may influence cellular viability through  
 230 processes including anti-proliferation and cell death [35,36], cell apoptosis has been  
 231 adopted as a vehicle for cancer treatment [37]. We next evaluated the apoptotic

232 activity of **C4**-treated MDA-MB-231 cells by means of Annexin-V and PI double  
 233 staining using a FACSCalibur flow cytometer. During apoptosis, phosphatidylserine  
 234 (PS) is translocated from the cytoplasmic face of the plasma membrane to the cell  
 235 surface. Thus, apoptotic cells can be identified by the presence of PS on the cell  
 236 surface. Annexin V has a strong  $\text{Ca}^{2+}$ -dependent affinity for PS, and therefore can be  
 237 used as a probe for detecting apoptosis. PI can only pass through the membranes of  
 238 later apoptotic and necrotic cells, and consequently intercalate into their nucleic acids,  
 239 since the integrity of their plasma and nuclear membranes was decreased. This allows  
 240 apoptotic cells (annexin-V<sup>+</sup>/PI<sup>-</sup> and annexin-V<sup>+</sup>/PI<sup>+</sup>) to be distinguished from living  
 241 (annexin-V<sup>-</sup>/PI<sup>-</sup>) and necrotic (annexin-V<sup>-</sup>/PI<sup>+</sup>) cells in flow cytometry analysis.



242

243 **Fig. 4.** a) Apoptosis of MDA-MB-231 cells induced by the **C4** (0, 0.25 × IC<sub>50</sub>, 0.5 × IC<sub>50</sub>, 1 ×

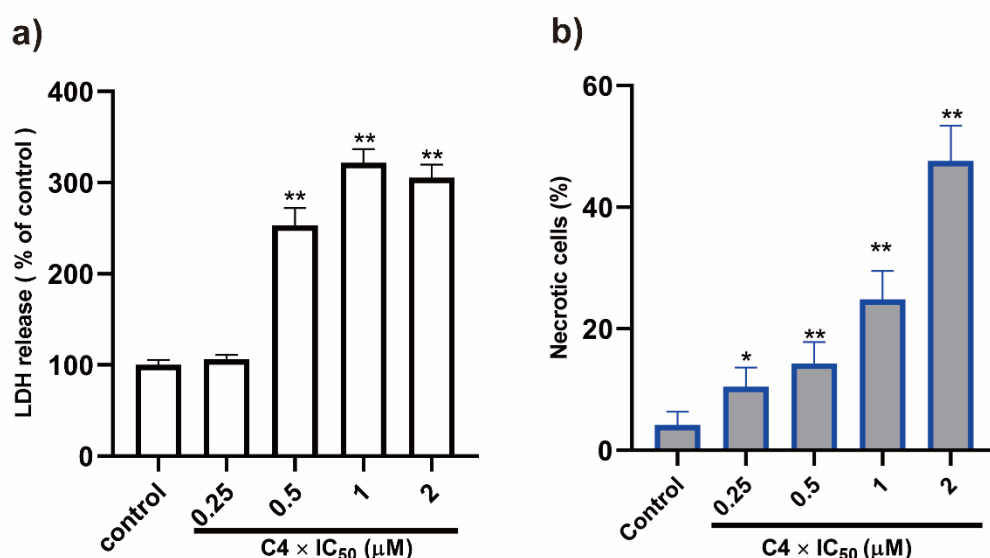
244  $IC_{50}$ , and  $1 \times IC_{50}$ ) for 48 h. b) All data were obtained from three independent experiments  
245 and presented as the mean  $\pm$  S.D. \* $P < 0.05$ , \*\* $P < 0.01$  compared with control.

246 In MDA-MB-231 cells incubated with compound **C4** at a 0.25 equipotent  
247 concentration of  $IC_{50}$  for 48 h, the proportion of apoptotic (early + late) cells  
248 increased to 2.07%, relatively slight compared to that of DMSO alone (1.51%). In  
249 contrast, even at a low **C4** dosage of 0.23  $\mu$ M, the treatment resulted in 10.43% of the  
250 MDA-MB-231 cells becoming necrotic, obviously higher than the 2.81% value of  
251 necrotic cells in untreated control (Fig. 4). With the increase of **C4** dosage to 0.5, 1,  
252 and 2 equipotent concentrations of  $IC_{50}$ , there was dose-dependent enhancement of  
253 both apoptotic (early + late) and necrotic cells to 8.76% and 38.88%, respectively. It is  
254 apparent that the main cause of cell death in human breast adenocarcinoma was the  
255 necrosis induced by compound **C4**.

#### 256 2.2.4 Lactate dehydrogenase release assay

257 Lactate dehydrogenase (LDH) is a stable cytoplasmic enzyme that is found in all  
258 cells. The leaking of LDH enzyme from the cytosol into the surrounding culture  
259 medium is generally regarded as an indicator of necrosis, and reflects a loss of  
260 membrane integrity in dead cells [38]. Because compound **C4** failed to significantly  
261 induce apoptosis, while the Annexin V-FITC/propidium iodide staining revealed that  
262 **C4** induced necrosis robustly, an LDH release assay was performed to further  
263 investigate the effects of **C4** on the LDH activity of treated MDA-MB-231 cells as  
264 specified in the experimental section. After treatment of MDA-MB-231 cells with  
265 compound **C4** (0.23, 0.46, 0.91, and 1.82  $\mu$ M for 48 h), there was somewhat elevation

266 of LDH release levels in the culture medium (Fig. 5a). Especially in the cases where  
 267 the cancerous cells were exposed to **C4** at concentration of 0.91 and 1.82  $\mu\text{M}$ , the  
 268 levels of LDH release were almost 3.21 and 3.05 fold ( $P < 0.01$ ) higher than that in  
 269 non-treated supernatant, respectively. With the increased levels of LDH release, we  
 270 confirmed that the necrosis of MDA-MB-231 cells was induced by **C4**.



271  
 272 **Fig. 5.** a) LDH release from MDA-MB-231 cells treated with different concentrations of **C4**  
 273 for 48 h. b) MDA-MB-231 cells treated with various concentrations of **C4** for 48 h, and the  
 274 necrotic cells were counted by Trypan blue exclusion assay. The values are presented as mean  
 275  $\pm$  S.D. of three independent experiments. \* $P < 0.05$ , \*\* $P < 0.01$ .

### 276 2.2.5 Trypan blue exclusion assay

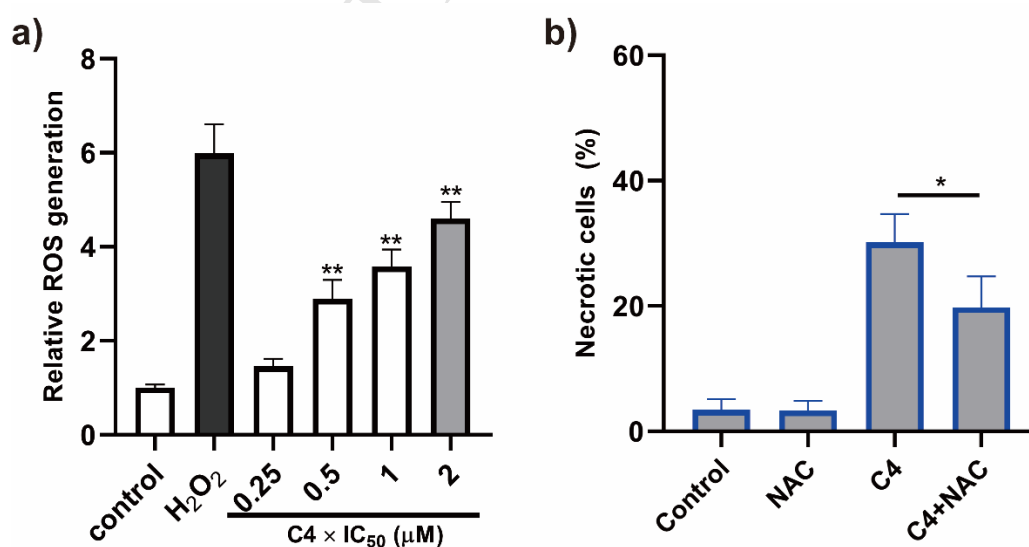
277 The Trypan blue dye exclusion test was used to determine the number of viable  
 278 cells present in a cell suspension. It is based on the principle that live cells will  
 279 exclude membrane-impermeable dyes such as trypan blue, whereas trypan blue can  
 280 penetrate inside necrotic cells and stain them [39,40]. In the present study, after  
 281 independent treatment with **C4** at concentrations of 0.23, 0.46, 0.91, and 1.82  $\mu\text{M}$  for  
 282 48 h, the MDA-MB-231 cells were trypsinized and stained with 0.2% Trypan blue

283 solution at 1:1 dilution for 5 min, and, thereafter, loaded into a hemocytometer for  
284 separate counting of stained (necrotic) and unstained (viable) cells. As shown in Fig.  
285 5b, complex **C4** dramatically induced necrosis in a dose-dependent manner, and  
286 almost 50% of MDA-MB-231 cells was identified with necrosis after **C4** (1.82  $\mu$ M)  
287 incubation of 48 h, which is in a agreement with the results presented in Fig. 4 and  
288 Fig. 5a. With such notation, the necrosis induced by antimonial **C4** has been  
289 repeatedly proven.

#### 290 2.2.6 Reactive oxygen species (ROS) assay

291 Reactive oxygen species (ROS) are radicals, ions or molecules that have a single  
292 unpaired electron in their outermost shell of electrons. Recent evidence has shown  
293 that ROS play a key role as a messenger for signal transduction and cell cycling in  
294 normal cells. However, unnecessary increases of ROS could result in cell death [41].  
295 Previous works revealed that metal-based chemotherapeutic agents (e.g. cisplatin)  
296 induced apoptosis and/or necrosis through ROS generation in several cancer cell lines  
297 [34,42]. It is widely accepted that the anticancer effect of these chemotherapeutics is  
298 due to the induction of oxidative stress and ROS-mediated cell injury in cancer. To  
299 explore whether cell necrosis induced by **C4** was dependent on the level of ROS, we  
300 assessed the production of intracellular ROS in **C4**-treated MDA-MB-231 cells by  
301 using 5-(and-6)-carboxy-2',7'-dichlorodihydrofluorescein diacetate (DCFH-DA) as  
302 fluorescence probe and H<sub>2</sub>O<sub>2</sub> as a positive control. Intracellular ROS levels were  
303 measured and quantified by change in relative fluorescence units (RFU). As shown in

304 Fig. 6a, compared to the negative untreated control, treatment with **C4** at graded  
 305 concentrations induced a significant elevation of ROS production in a dose-dependent  
 306 manner. When the exposure was 1.82  $\mu\text{M}$  for 48 h, **C4** promoted an increase of 4.61  
 307 fold ( $P < 0.01$ ) of ROS production compared to that of untreated control. The  
 308 excessive increase of ROS production in cells might be attributed to the cytotoxic  
 309 activity of compound **C4** through the activation of mitochondria-initiated events.  
 310 Furthermore, we examined the effect of *N*-acetylcysteine (NAC), a well-known  
 311 antioxidant, on the necrotic activity of **C4**-treated MDA-MB-231 cells by means of  
 312 Trypan blue dye exclusion test, as shown in Fig 6b. After pretreatment with NAC (5  
 313  $\mu\text{M}$ ) for 2 h, the population of necrotic MDA-MB-231 cells induced by **C4** was  
 314 significantly decreased from 30.16% to 19.79%, evidencing the retarding effect of  
 315 NAC. It is consistent with the notion that the **C4**-driven induction of necrosis in  
 316 MDA-MB-231 cells is dependent on the production of intracellular ROS.



317  
 318 **Fig. 6.** a) ROS generation in **C4** treated MDA-MB-231 cells. Relative fluorescence units  
 319 (RFU) of DCF was measured using a spectrofluorometer with excitation at 485 nm and  
 320 emission at 530 nm. b) Cells were pretreated with NAC (5  $\mu\text{M}$ ) for 2 h, followed by treatment

321 with an IC<sub>50</sub> concentration of **C4** (0.91 μM) for 48 h before determination of cell death by  
322 Trypan blue dye exclusion assay. The results are presented as mean ± S.D. (\**P* < 0.05, \*\**P* <  
323 0.01).

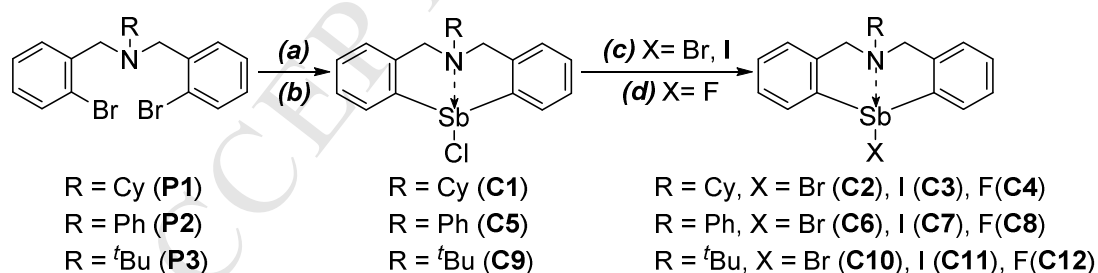
ACCEPTED MANUSCRIPT

### 324 3. Conclusion

325 In the present study, a series of organoantimony(III) halide complexes with  
326 azastibocine framework were synthesized, characterized and evaluated for *in vitro*  
327 cytotoxic activity on human liver hepatocellular carcinoma cell line (HepG2), human  
328 breast cancer cell line (MDA-MB-231), human breast adenocarcinoma cell line  
329 (MCF-7), human cervical carcinoma cell line (HeLa) and human embryonic kidney  
330 cell line (HEK-293). The results reveal a positive correlation between cytotoxic  
331 activity and the N→Sb coordinate bond lengths in the complexes with same nitrogen  
332 substituent. Among all tested trivalent organoantimony complexes, the complex  
333 6-cyclohexyl-12-fluoro-5,6,7,12-tetrahydrodibenzo[*c,f*][1,5]azastibocine (C4)  
334 exhibited the highest selectivity index. Further mechanistic investigation indicated  
335 that C4 causes cell cycle arrest mainly at the S phase, and consequently results in  
336 necrosis of MDA-MB-231 cells through the production of intracellular reactive  
337 oxygen species. The results indicate that the azastibocine-framework organoantimony  
338 halide complexes could be promising candidates for the development of new drugs in  
339 cancer therapy. Specifically, the elucidation of correlation between cytotoxicity and  
340 intermolecular interaction has provided theoretical and experimental basis for  
341 in-depth design of antimony-based antineoplastic metallodrugs.

342 **4. Experimental**343 *4.1. Chemistry*

344 The commercially available starting materials were purchased from Adamas-beta,  
 345 and were used as received unless otherwise noted. The preparation of *N*-containing  
 346 precursors (**P1–P3**) and organoantimony(III) chlorides (**C1**, **C4** and **C9**) were  
 347 prepared according to literature procedures [30,43]. Melting points were determined  
 348 over a XT-4 micro melting point apparatus (Beijing Tech Instrument Co., Ltd.).  
 349 Nuclear magnetic resonance (NMR) data were obtained on a Bruker-400 spectrometer  
 350 (400 MHz for <sup>1</sup>H, 100 MHz for <sup>13</sup>C and 376 MHz for <sup>19</sup>F spectroscopy). Chemicals  
 351 shifts are reported in ppm (δ) relative to internal tetramethylsilane (TMS). In this  
 352 paper, data are reported as follows: Chemical shift, multiplicity (s = singlet, d =  
 353 doublet, t = triplet, q = quartet, m = multiplet). Coupling constants (*J*) are reported in  
 354 hertz. Elemental analyses were performed using a VARIO EL III instrument.



355

356 **Scheme 1.** Synthesis of organoantimony(III) halide complexes **C1–C12**. (a) <sup>n</sup>BuLi (2.0  
 357 equiv.), Et<sub>2</sub>O, -60 °C to room temperature. (b) SbCl<sub>3</sub> (1.1 equiv.), Et<sub>2</sub>O, -78 °C to room  
 358 temperature; **C1**, 72%; **C5**, 78%; **C9**, 80%. (c) KBr or KI (10.0 equiv.), CH<sub>2</sub>Cl<sub>2</sub>/H<sub>2</sub>O, room  
 359 temperature; **C2**, 92%; **C3**, 86%; **C6**, 87%; **C7**, 85%; **C10**, 91%; **C11**, 81%. (d) AgF (1.0  
 360 equiv.), CH<sub>2</sub>Cl<sub>2</sub>/H<sub>2</sub>O, room temperature, dark; **C4**, 93%; **C8**, 95%; **C12**, 76%.

361 *4.1.1. General procedure for the synthesis of organoantimony(III) chlorides*

362 To a solution of *N*-containing precursors (25 mmol) in anhydrous ether (100 mL),  
363 *n*-BuLi in hexane (2.5 M, 20 mL) was added dropwise under nitrogen with vigorous  
364 stirring at -30 °C, and the mixture thus obtained was warmed to room temperature for  
365 3 h. Then a solution of SbCl<sub>3</sub> (5.8 g, 25.5 mmol) in anhydrous ether (60 mL) was  
366 added slowly at -78 °C within 30 min. After subject to stirring at room temperature  
367 overnight, the solution was subject to evaporation under reduced pressure. The  
368 residue was extracted with dichloromethane (100 mL) and washed with a solution of  
369 NH<sub>4</sub>Cl (1M) in H<sub>2</sub>O. The organic layer was washed with deionized water (3 × 50  
370 mL), dried over anhydrous Na<sub>2</sub>SO<sub>4</sub>, subject to filtration, and concentrated in vacuo.  
371 The residue was purified by recrystallization in CH<sub>2</sub>Cl<sub>2</sub>/*n*-hexane mixture to afford  
372 the corresponding organoantimony chloride as colorless crystals.

#### 373 4.1.2. General procedure for the synthesis of organoantimony(III) bromides

374 To a solution of organoantimony chloride (5.0 mmol) in CH<sub>2</sub>Cl<sub>2</sub> (30 mL), a solution  
375 of KBr (6.0 g, 50 mmol) in deionized water (25 mL) was added under open-flask  
376 conditions. After being stirred at room temperature overnight, the solution was  
377 extracted with CH<sub>2</sub>Cl<sub>2</sub> (3 × 30 mL). The combined organic layer was dried over  
378 anhydrous Na<sub>2</sub>SO<sub>4</sub>, and subject to filtration. The filtrate was mixed with *n*-hexane and  
379 kept at room temperature for 24 h to afford the corresponding organoantimony  
380 bromide as colorless crystals.

#### 381 4.1.3. General procedure for the synthesis of organoantimony(III) iodides

382 To a solution of organoantimony chloride (5.0 mmol) in CH<sub>2</sub>Cl<sub>2</sub> (30 mL), a solution  
383 of KI (8.3 g, 50 mmol) in deionized water (25 mL) was added under open-flask

384 conditions. After subject to stirring at room temperature overnight, the solution was  
385 extracted with CH<sub>2</sub>Cl<sub>2</sub> (3 × 30 mL). The combined organic layer was dried over  
386 anhydrous Na<sub>2</sub>SO<sub>4</sub>, and subject to filtration. The filtrate was mixed with *n*-hexane and  
387 kept at room temperature for 24 h to afford the corresponding organoantimony iodide  
388 as colorless crystals.

#### 389 4.1.4. General procedure for the synthesis of organoantimony(III) fluorides

390 To a solution of organoantimony chloride (5.0 mmol) in CH<sub>2</sub>Cl<sub>2</sub> (30 mL), a  
391 solution of AgF (635 mg, 5.0 mmol) in deionized water (25 mL) was added  
392 under open-flask conditions. After being stirred in the dark at room temperature  
393 for 4 h, the mixture was subject to filtration. The filtrate was mixed with  
394 *n*-hexane and kept at room temperature for 24 h to afford the corresponding  
395 organoantimony fluoride as colorless crystals.

#### 396 4.1.5. Analytical data for the synthesized organoantimony halide complexes

397 *12-chloro-6-cyclohexyl-5,6,7,12-tetrahydrodibenzo[c,f][1,5]azastibocine* (C1).

398 Yield: 72% (7.8 g). Melting point: 254–256 °C. <sup>1</sup>H NMR (400 MHz, CDCl<sub>3</sub>, TMS): δ  
399 8.30 (2H, d, *J* = 7.4 Hz), 7.39–7.27 (4H, m), 7.14 (2H, d, *J* = 7.4 Hz), 4.15 (4H, dd, *J*  
400 = 61.9, 15.1 Hz), 3.09 (1H, t, *J* = 11.3 Hz), 2.05 (2H, d, *J* = 11.7 Hz), 1.86 (2H, d, *J* =  
401 12.5 Hz), 1.69 (d, *J* = 13.0 Hz), 1.46–1.27 (m, 4H), 1.18–1.08 (m, 1H); <sup>13</sup>C NMR  
402 (100 MHz, CDCl<sub>3</sub>, TMS): δ 144.0, 140.1, 134.9, 128.8, 128.7, 124.7, 65.4, 57.8, 29.5,  
403 25.6, 25.4. Anal. Calc. for C<sub>20</sub>H<sub>23</sub>ClNSb: C, 55.27; H, 5.33; N, 3.22. Found: C, 55.39;  
404 H, 5.25; N, 3.14.

405 *12-bromo-6-cyclohexyl-5,6,7,12-tetrahydrodibenzo[c,f][1,5]azastibocine* (C2).

406 Yield: 92% (2.2 g). Melting point: 245–247 °C. <sup>1</sup>H NMR (400 MHz, CDCl<sub>3</sub>, TMS): δ  
407 8.40–8.38 (2H, m), 7.37–7.27 (4H, m), 7.13 (2H, d, *J* = 6.6 Hz), 4.15 (4H, dd, *J* =  
408 58.0, 15.1 Hz), 3.13–3.08 (1H, m), 2.04 (2H, d, *J* = 10.9 Hz), 1.85 (2H, d, *J* = 11.8  
409 Hz), 1.68 (1H, d, *J* = 11.8 Hz), 1.45–1.27 (4H, m), 1.17–1.09 (1H, m); <sup>13</sup>C NMR (100  
410 MHz, CDCl<sub>3</sub>, TMS): δ 144.0, 138.0, 136.3, 128.9, 128.7, 124.7, 65.5, 57.8, 29.6, 25.6,  
411 25.4. Anal. Calc. for C<sub>20</sub>H<sub>23</sub>BrNSb: C, 50.14; H, 4.84; N, 2.92. Found: C, 50.29; H,  
412 4.95; N, 2.99.

413 *6-cyclohexyl-12-iodo-5,6,7,12-tetrahydrodibenzo[c,f][1,5]azastibocine (C3)*. Yield:  
414 86% (2.3 g). Melting point: 253–255 °C. <sup>1</sup>H NMR (400 MHz, CDCl<sub>3</sub>, TMS): δ 8.52  
415 (2H, d, *J* = 7.0 Hz), 7.39–7.30 (4H, m), 7.12 (2H, d, *J* = 6.9 Hz), 4.14 (4H, dd, *J* =  
416 52.4, 15.0 Hz), 3.12 (1H, t, *J* = 11.4 Hz), 2.07 (2H, d, *J* = 11.2 Hz), 1.88 (2H, d, *J* =  
417 12.4 Hz), 1.71 (1H, d, *J* = 13.2 Hz), 1.47–1.31 (4H, m), 1.19–1.13 (1H, m); <sup>13</sup>C NMR  
418 (100 MHz, CDCl<sub>3</sub>, TMS): δ 143.8, 139.4, 134.5, 129.2, 129.0, 124.7, 65.6, 57.6, 29.7,  
419 25.7, 25.4. Anal. Calc. for C<sub>20</sub>H<sub>23</sub>INSb: C, 45.66; H, 4.41; N, 2.66. Found: C, 45.74;  
420 H, 4.54; N, 2.79.

421 *6-cyclohexyl-12-fluoro-5,6,7,12-tetrahydrodibenzo[c,f][1,5]azastibocine (C4)*.  
422 Yield: 93% (1.9 g). Melting point: 237–239 °C. <sup>1</sup>H NMR (400 MHz, CDCl<sub>3</sub>,  
423 TMS): δ 7.97 (2H, d, *J* = 7.3 Hz), 7.40–7.25 (4H, m), 7.14 (2H, t, *J* = 7.4 Hz),  
424 4.09 (4H, dd, *J* = 71.4, 15.2 Hz), 3.03 (1H, t, *J* = 10.8 Hz), 2.00 (2H, d, *J* = 11.4  
425 Hz), 1.86 (2H, d, *J* = 12.5 Hz), 1.69 (2H, d, *J* = 12.7 Hz), 1.45–1.26 (4H, m),  
426 1.18–1.09 (1H, m); <sup>13</sup>C NMR (100 MHz, CDCl<sub>3</sub>, TMS): δ 144.1, 144.0 (d, *J* =  
427 6.4 Hz), 133.4 (d, *J* = 6.0 Hz), 128.5, 128.3, 124.7, 65.2, 57.7 (d, *J* = 2.1 Hz),

428 29.5, 25.7, 25.5;  $^{19}\text{F}$  NMR (376 MHz,  $\text{CDCl}_3$ ):  $\delta$  -185.45. Anal. Calc. for  
429  $\text{C}_{20}\text{H}_{23}\text{FNSb}$ : C, 57.45; H, 5.54; N, 3.35. Found: C, 57.53; H, 5.59; N, 3.44. FT-IR  
430 (KBr,  $\text{cm}^{-1}$ ):  $\nu$  2935, 2857, 1455, 1440, 1268, 1204, 1100, 975, 950, 934, 896, 758.

431 *12-chloro-6-phenyl-5,6,7,12-tetrahydrodibenzo[c,f][1,5]azastibocine (C5)*. Yield:  
432 76% (8.1 g). Melting point: 222–224 °C.  $^1\text{H}$  NMR (400 MHz,  $\text{CDCl}_3$ , TMS):  $\delta$  8.40–  
433 8.28 (2H, m), 7.47–7.42 (2H, m), 7.38–7.34 (4H, m), 7.30–7.19 (5H, m), 4.66 (4H, dd,  
434  $J = 70.8, 14.9$  Hz);  $^{13}\text{C}$  NMR (100 MHz,  $\text{CDCl}_3$ , TMS):  $\delta$  147.9, 143.1, 140.5, 135.2,  
435 129.5, 129.2, 129.2, 125.4, 125.3, 119.7, 61.2. Anal. Calc. for  $\text{C}_{20}\text{H}_{17}\text{ClNSb}$ : C, 56.05;  
436 H, 4.00; N, 3.27. Found: C, 55.73; H, 4.12; N, 3.35.

437 *12-bromo-6-phenyl-5,6,7,12-tetrahydrodibenzo[c,f][1,5]azastibocine (C6)*. Yield:  
438 87% (2.0 g). Melting point: 233–235 °C.  $^1\text{H}$  NMR (400 MHz,  $\text{CDCl}_3$ , TMS):  $\delta$  8.41–  
439 8.29 (2H, m), 7.47–7.43 (2H, m), 7.40–7.35 (4H, m), 7.31–7.29 (2H, m), 7.25–7.21  
440 (3H, m), 4.67 (4H, dd,  $J = 65.7, 14.9$  Hz);  $^{13}\text{C}$  NMR (100 MHz,  $\text{CDCl}_3$ , TMS)  $\delta$  147.8,  
441 143.0, 138.2, 136.8, 129.6, 129.4, 129.3, 125.5, 125.3, 119.8, 61.2. Anal. Calc. for  
442  $\text{C}_{20}\text{H}_{17}\text{BrNSb}$ : C, 50.78; H, 3.62; N, 2.96. Found: C, 50.89; H, 3.69; N, 3.07.

443 *12-iodo-6-phenyl-5,6,7,12-tetrahydrodibenzo[c,f][1,5]azastibocine (C7)*. Yield:  
444 85% (2.2 g). Melting point: 249–251 °C.  $^1\text{H}$  NMR (400 MHz,  $\text{CDCl}_3$ , TMS):  $\delta$   
445 8.47–8.45 (2H, m), 7.39–7.30 (6H, m), 7.26–7.23 (2H, m), 7.19–7.16 (3H, m),  
446 4.60 (4H, dd,  $J = 66.6, 14.9$  Hz);  $^{13}\text{C}$  NMR (100 MHz,  $\text{CDCl}_3$ , TMS):  $\delta$  147.6,  
447 142.9, 140.0, 134.1, 129.6, 129.5, 129.4, 125.5, 125.3, 119.8, 60.9. Anal. Calc.  
448 for  $\text{C}_{20}\text{H}_{17}\text{INSb}$ : C, 46.19; H, 3.30; N, 2.69. Found: C, 46.27; H, 3.33; N, 2.76.

449 *12-fluoro-6-phenyl-5,6,7,12-tetrahydrodibenzo[c,f][1,5]azastibocine (C8)*. Yield:  
450 95% (2.0 g). Melting point: 216–218 °C. <sup>1</sup>H NMR (400 MHz, CDCl<sub>3</sub>, TMS): δ  
451 8.00 (2H, d, *J* = 7.3 Hz), 7.46 (2H, t, *J* = 7.3 Hz), 7.35–7.34 (4H, m), 7.20–7.25  
452 (4H,m), 7.20 (1H, t, *J* = 6.8 Hz), 4.63 (4H, dd, *J* = 85.1, 15.0 Hz); <sup>13</sup>C NMR  
453 (100 MHz,CDCl<sub>3</sub>, TMS): δ 148.5, 144.7 (d, *J* = 6.6 Hz), 143.1, 133.4 (d, *J* =  
454 6.2 Hz), 129.5, 128.9, 128.8, 125.2, 125.0, 119.4, 61.2 (d, *J* = 1.8 Hz); <sup>19</sup>F  
455 NMR (376 MHz, CDCl<sub>3</sub>): δ -198.97. Anal. Calc. for C<sub>20</sub>H<sub>17</sub>FNSb: C, 58.29; H,  
456 4.16; N, 3.40. Found: C, 58.39; H, 4.24; N, 3.58.

457 *6-(tert-butyl)-12-chloro-5,6,7,12-tetrahydrodibenzo[c,f][1,5]azastibocine (C9)*.  
458 Yield: 80% (8.1 g). Melting point: 213–215 °C. <sup>1</sup>H NMR (400 MHz, CDCl<sub>3</sub>, TMS): δ  
459 8.32 (2H, d, *J* = 7.3 Hz), 7.37 (2H, t, *J* = 7.2 Hz), 7.31–7.28 (2H, m), 7.15 (2H, d, *J* =  
460 7.5 Hz), 4.23 (4H, dd, *J* = 161.2, 15.4 Hz), 1.38 (9H, s); <sup>13</sup>C NMR (100 MHz,CDCl<sub>3</sub>,  
461 TMS): δ 145.1, 139.9, 134.9, 128.9, 128.4, 124.5, 60.4, 57.2, 27.0. Anal. Calc. for  
462 C<sub>18</sub>H<sub>21</sub>ClNSb: C, 52.91; H, 5.18; N, 3.43. Found: C, 52.78; H, 5.26; N, 3.52.

463 *12-bromo-6-(tert-butyl)-5,6,7,12-tetrahydrodibenzo[c,f][1,5]azastibocine (C10)*.  
464 Yield: 91% (2.0 g). Melting point: 244–246 °C. <sup>1</sup>H NMR (400 MHz, CDCl<sub>3</sub>, TMS):  
465 δ 8.41 (2H, d, *J* = 7.2 Hz), 7.36–7.27 (4H, m), 7.15 (2H, d, *J* = 6.8 Hz), 4.22 (4H, dd,  
466 *J* = 152.9, 15.4 Hz), 1.37 (9H, s); <sup>13</sup>C NMR (100 MHz,CDCl<sub>3</sub>, TMS): δ 145.0, 137.8,  
467 136.4, 129.0, 128.5, 124.5, 60.6, 57.2, 27.1. Anal. Calc. for C<sub>18</sub>H<sub>21</sub>BrNSb: C, 47.72; H,  
468 4.67; N, 3.09. Found: C, 47.82; H, 4.75; N, 3.16.

469 *6-(tert-butyl)-12-iodo-5,6,7,12-tetrahydrodibenzo[c,f][1,5]azastibocine (C11)*.  
470 Yield: 81% (2.0 g). Melting point: 228–230 °C. <sup>1</sup>H NMR (400 MHz, CDCl<sub>3</sub>,

471 TMS):  $\delta$  8.54–8.51 (2H, m), 7.34–7.30 (4H, m), 7.12–7.10 (2H, m), 4.20 (4H,  
472 dd,  $J$  = 151.4, 15.3 Hz), 1.38 (9H, s);  $^{13}\text{C}$  NMR (100 MHz,  $\text{CDCl}_3$ , TMS):  $\delta$   
473 144.9, 139.6, 134.3, 129.2, 128.8, 124.5, 60.8, 57.1, 27.2. Anal. Calc. for  
474  $\text{C}_{18}\text{H}_{21}\text{INSb}$ : C, 43.24; H, 4.23; N, 2.80. Found: C, 43.33; H, 4.35; N, 2.96.

475 *6-(tert-butyl)-12-fluoro-5,6,7,12-tetrahydridibenzo[c,f][1,5]azastibocine* (**C12**).  
476 Yield: 76% (1.5 g). Melting point: 206–208 °C.  $^1\text{H}$  NMR (400 MHz,  $\text{CDCl}_3$ ,  
477 TMS):  $\delta$  7.80 (2H, d,  $J$  = 7.3 Hz), 7.16 (2H, t,  $J$  = 7.3 Hz), 7.07 (2H, t,  $J$  = 7.3  
478 Hz), 6.96 (2H, d,  $J$  = 7.7 Hz), 3.95 (4H, dd,  $J$  = 171.1, 15.4 Hz), 1.13 (9H, s);  
479  $^{13}\text{C}$  NMR (100 MHz,  $\text{CDCl}_3$ , TMS):  $\delta$  145.1, 143.8 (d,  $J$  = 5.8 Hz), 133.2 (d,  $J$   
480 = 6.5 Hz), 128.5, 128.0, 124.5, 59.7, 57.1, 26.9;  $^{19}\text{F}$  NMR (376 MHz,  $\text{CDCl}_3$ ):  $\delta$   
481 -185.16. Anal. Calc. for  $\text{C}_{18}\text{H}_{21}\text{FNSb}$ : C, 55.13; H, 5.40; N, 3.57. Found: C, 52.25; H,  
482 5.46; N, 3.62.

#### 483 4.1.6. X-ray crystal structural determination of organoantimony(III) halide complexes

#### 484 **C1–C12**

485 X-ray crystal structural determination of complexes **C1**, **C5**, and **C9** have described  
486 previously [30]. X-ray single crystal diffraction analysis of these complexes was  
487 performed at Hunan University using a Bruker SMART APEX diffractometer. The  
488 CDCC number is 1864560 (**C2**), 1859257 (**C3**), 1859365 (**C4**), 945750 (**C6**), 945752  
489 (**C7**), 769426 (**C8**), 1861311 (**C10**), 1859366 (**C11**), 1864561 (**C12**), respectively. In  
490 all cases, the diffraction data were collected using graphite monochromated Mo- $\text{K}\alpha$   
491 radiation ( $\lambda$  = 0.71073 Å). The collected frames were processed with SAINT+  
492 software and the collected reflections were subject to absorption correction

493 (SADABS) [44]. The structure was solved by the Direct method (SHELXTL) in  
494 conjunction with standard difference Fourier techniques and subsequently refined by  
495 full-matrix least-squares analyses on  $F^2$  [45]. The hydrogen atoms were generated in  
496 their idealized positions and all non-hydrogen atoms were refined anisotropically (see  
497 Table 2).

## 498 4.2. Biological evaluation

### 499 4.2.1. Cell lines and cell culture

500 Human cancerous cell lines: HepG2 (human liver hepatocellular carcinoma cell  
501 line), MDA-MB-231 (human breast cancer cell line), MCF-7 (human breast  
502 adenocarcinoma cell line), HeLa (human cervical carcinoma cell line) and  
503 nonmalignant cell lines: HEK-293 (human embryonic kidney cell line) used in this  
504 study were supplied by the Cancer Research Institute, Central South University  
505 (Changsha, Hunan, PR China). The cells were cultivated in Dulbecco's modified  
506 Eagle's medium (DMEM, Gibco) or RPMI (HyClone), supplemented with 10% fetal  
507 bovine serum containing L-glutamine and 1% penicillin-streptomycin (HyClone) and  
508 maintained in a humidified atmosphere of 95% air, 5% CO<sub>2</sub> at 37°C.

### 509 4.2.2. Cell viability

510 The cell viability of the organometallic complexes in cells was determined by the  
511 CCK-8 assay (Dojindo Molecular Technologies, Shanghai, China) using a modified  
512 method as previously described [46]. Each of the tested organoantimony complexes  
513 was completely dissolved in DMSO to a solution of 10 mM. Briefly,  $5 \times 10^3$  cells

514 were seeded in each well of the 96-well plates with fresh medium. After complete  
515 adhesion, the cells were continuously exposed to test complexes of 0.01, 0.3, 1, 3 and  
516 10  $\mu$ M for 24 h. A CCK-8 solution (10  $\mu$ L) was added and the plates were incubated  
517 at 37 °C for a further 2 h. Subsequently, the absorbance of formazan yellow formed in  
518 the cells was measured at 450 nm, using an iMark microplate absorbance reader  
519 (Bio-Rad, USA). The IC<sub>50</sub> values were determined by the four-parameter logistic  
520 method. Mean IC<sub>50</sub> values were obtained from at least three independent experiments.

#### 521 4.2.3. Cell cycle analysis

522 Complex **C4** on the cell cycle perturbation in MDA-MB-231 cells was examined  
523 by flow cytometry analysis. Briefly,  $1.0 \times 10^6$  per well were seeded in a six-well  
524 plate. After treated with  $0.25 \times \text{IC}_{50}$ ,  $0.5 \times \text{IC}_{50}$ ,  $1 \times \text{IC}_{50}$  and  $2 \times \text{IC}_{50}$  of **C4** for 24 h,  
525 the supernatants were removed and cells were washed with PBS. The cells were  
526 subsequently harvested by trypsinization, then fixed and stained with PI (Cat. no.  
527 537059, Calbiochem, San Diego, CA, USA). This was followed by the measurement  
528 of propidium-iodide-mediated fluorescence with flow cytometry (FACSCalibur BD,  
529 Bedford, MA, USA) by using excitation of DNA-bound PI at 488 nm, with emission  
530 at 585 nm. The cell cycle distribution is shown as the percentage of cells containing  
531  $G_0/G_1$ , S and  $G_2/M$  DNA as identified by PI staining.

#### 532 4.2.4. Apoptosis Analysis

533 For apoptosis assay, cells were stained with Annexin V-FITC and PI Kit (Cat. no.  
534 LOT9104010102, Dinguo Bio. Inc., Beijing, China) as previously described [30].  
535 Briefly, MDA-MB-231 cells were incubated with complexes as indicated in the

536 figures for 48 h. At the end of incubation, the cells were harvested and washed twice  
537 in PBS, then re-suspended in 500  $\mu$ L of binding buffer and incubated with 5  $\mu$ L of  
538 annexin V-FITC and 5  $\mu$ L of PI for 15 min at room temperature in the dark. Flow  
539 cytometry was performed on a FACS Calibur<sup>TM</sup> flow cytometer and the collected  
540 data were analyzed using FlowJo software (Becton, Dickinson & Company). The  
541 results were interpreted as follows: cells in the lower left quadrant (annexin-V<sup>-</sup>/PI<sup>-</sup>)  
542 were considered as living cells, in the lower right quadrant (annexin-V<sup>+</sup>/PI<sup>-</sup>) as early  
543 apoptotic cells, in the upper right quadrant (annexin-V<sup>+</sup>/PI<sup>+</sup>) as late apoptotic cells,  
544 and in the upper left quadrant (annexin-V<sup>-</sup>/PI<sup>+</sup>) as necrotic cells. The total apoptotic  
545 rate was the rate of cells in the lower right quadrant (annexin-V<sup>+</sup>/PI<sup>-</sup>) plus that in the  
546 upper right quadrant (annexin-V<sup>+</sup>/PI<sup>+</sup>).

#### 547 4.2.5. Lactate dehydrogenase (LDH) release assay

548 The LDH activity of treated MDA-MB-231 cells was monitored according to the  
549 manufacturer's instructions (Cat. no. C0016, Beyotime, Haimen, China). Briefly,  
550 treated cells with diverse concentrations of complex C4 were incubated for 48 hours.  
551 Next, the medium was centrifuged at 2000 rpm for 5 min to obtain the supernatant.  
552 The supernatant was transferred to a new 96-well plate. Then 100  $\mu$ l of the LDH  
553 reaction was added to each well and was incubated for 30 min at room temperature  
554 before absorbance measurement using an iMark microplate absorbance reader  
555 (Bio-Rad, USA) at 490 nm.

#### 556 4.2.6. Trypan blue dye exclusion assay

557 MDA-MB-231 cells (  $5 \times 10^4$  ) were seeded in 12-well plates and exposed to

558 complex **C4** at the indicated concentrations as illustrated in the figures for 48 h. The  
559 cells were trypsinized and stained with 0.2% Trypan blue solution (Cat. no. SBJ-0245,  
560 Beyotime, China) at 1:1 dilution for 5 min, and were then loaded into a  
561 hemocytometer for separate counting of stained (necrotic) and unstained (viable)  
562 cells.

#### 563 4.2.7. Reactive oxygen species (ROS) assay

564 The production of intracellular ROS in **C4**-treated MDA-MB-231 cells was  
565 assessed using 2',7'-dichlorofluorescein diacetate (DCFH-DA) assay. The assay used  
566 the cell-permeable fluorogenic probe DCFH-DA, which upon diffusion into cells is  
567 oxidized by cellular ROS to form highly fluorescent 2',7'-dichlorodihydrofluorescein  
568 (DCF). H<sub>2</sub>O<sub>2</sub> was used as a positive control. The effects of **C4** on intracellular ROS  
569 production can be measured in terms of relative fluorescence units (RFU). Briefly,  
570 MDA-MB-231 cells were seeded in 6-well microplates, treated with complex **C4** as  
571 indicated in the figures for 48 h. After 48 h of **C4** treatment, the cells were washed  
572 twice with PBS and then incubated with the DCFH-DA probe (10 μM) at 37 °C for 30  
573 min, and then immediately washed three times with PBS. Fluorescence was measured  
574 with a BioTek ELx800 microplate reader at an excitation wavelength of 485 nm and  
575 an emission wavelength of 528 nm.

#### 576 4.2.8. Statistical analysis

577 Data were obtained from at least three separate experiments and the results were  
578 expressed as mean ± S.D. The data were analyzed for statistical significance by  
579 one-way ANOVA using GraphPad Prism version 7.0.5 for Windows, GraphPad

580 Software, San Diego, CA, USA., and  $p < 0.05$  was considered statistically significant  
581 (notation: \* $P < 0.05$ , \*\* $P < 0.01$ ).

ACCEPTED MANUSCRIPT

582 **Acknowledgments**

583 This work was supported by the National Natural Science Foundation of China  
584 (21571060, 21725602), and the Natural Science Foundation of Hunan Province  
585 (2018JJ2288, 2019JJ40222); C.-T. Au thanks HNU for an adjunct professorship.

586 **References**

- 587 [1] L. Ronconi, P.J. Sadler, Using coordination chemistry to design new medicines, *Coordin.*  
588 *Chem. Rev.* 251 (2007) 1633–1648.
- 589 [2] S. Komeda, A. Casini, Next-generation anticancer metallodrugs, *Curr. Top. Med. Chem.*  
590 12 (2012) 219–235.
- 591 [3] A.L. Lainé, C. Passirani, Novel metal-based anticancer drugs: a new challenge in drug  
592 delivery, *Curr. Opin. Pharmacol.* 12 (2012) 420–426.
- 593 [4] K.D. Mjos, C. Orvig, Metallodrugs in medicinal inorganic chemistry, *Chem. Rev.* 114  
594 (2014) 4540–4563.
- 595 [5] N. Muhammad, Z. Guo, Metal-based anticancer chemotherapeutic agents, *Curr. Opin.*  
596 *Chem. Biol.* 19 (2014) 144–153.
- 597 [6] F. Petrelli, S. Barni, G. Bregni, F. de Braud, S. Di Cosimo, Platinum salts in advanced  
598 breast cancer: a systematic review and meta-analysis of randomized clinical trials, *Breast*  
599 *Cancer Res. Treat.* 160 (2016) 425–437.
- 600 [7] J. Berman, Current treatment approaches to leishmaniasis, *Curr. Opin. Infect. Dis.* 16  
601 (2003) 397–401.
- 602 [8] M.N. Rocha, P.M. Nogueira, C. Demicheli, L.G. de Oliveira, M.M. da Silva, F. Frezard,  
603 M.N. Melo, R.P. Soares, Cytotoxicity and in vitro antileishmanial activity of antimony  
604 (V), Bismuth (V), and Tin (IV) complexes of lapachol, *Bioinorg. Chem. Appl.* 2013  
605 (2013) 961783–961789.
- 606 [9] E.R. Tiekink, Antimony and bismuth compounds in oncology. *Crit. Rev. Oncol. Hemat.*  
607 42 (2002) 217–224.
- 608 [10] B. DESOIZE, Metals and metal compounds in cancer treatment, *Anticancer Res.* 24  
609 (2004) 1529–1544.
- 610 [11] S. Muller, W.H. Miller, A. Dejean, Trivalent antimonials induce degradation of the  
611 PML-RAR oncoprotein and reorganization of the promyelocytic leukemia nuclear bodies  
612 in acute promyelocytic leukemia NB4 cells, *Blood* 92 (1998) 4308–4316.
- 613 [12] S.-Z. Hu, L.-D. Tu, Y.-Q. Huang, Z.-X. Li, Studies on the antitumor antimony(III)  
614 aminopolycarboxylic acid chelates. Crystal structures of  $M[\text{Sb}(\text{pdta})] \cdot \text{H}_2\text{O}$  ( $M = \text{Na}^+$ ,  
615  $\text{NH}_4^+$ ; pdta = propylenediaminetetraacetic acid), *Inorg. Chim. Acta* 232 (1995) 161–165.
- 616 [13] S.Z. Hu, Y.M. Fu, B. Xu, W.D. Tang, W.J. Yu, STUDIES ON THE ANTITUMOR  
617 ANTIMONY (III) TRIAMINOCARBOXYLIC COMPLEXONATES. CRYSTAL  
618 STRUCTURES OF  $\text{NH}_4[\text{Sb}(\text{Hdtpa})] \cdot \text{H}_2\text{O}$  AND  $\text{Na}[\text{Sb}(\text{Hdtpa})] \cdot 4_{1/2} \text{H}_2\text{O}$  (dtpa =  
619 DIETHYLENETRIAMINEPENTAACETIC ACID), *Main Group Met. Chem.* 20(1997)  
620 169–180.
- 621 [14] A.M. Popov, R.L. Davidovich, I.A. Li, A.V. Skul'beda, S.Z. Hu, Cytotoxic and  
622 Antitumor Activity of Antimony (III) Nitritotriacetate Complexes  
623  $\text{M}_2\text{SB}(\text{Nta})(\text{HNta}) \cdot n\text{H}_2\text{O}$  ( $M = \text{NH}_4, \text{Na}$ ;  $n = 1, 2$ ), *Pharm. Chem. J.* 39 (2005) 119–121.
- 624 [15] K.S.O. Ferraz, N.F. Silva, J.G. da Silva, L.F. de Miranda, C.F.D. Romeiro, E.M.  
625 Souza-Fagundes, I.C. Mendes, H. Beraldo, Investigation on the pharmacological profile  
626 of 2,6-diacetylpyridine bis(benzoylhydrazone) derivatives and their antimony(III) and  
627 bismuth(III) complexes, *Eur. J. Med. Chem.* 53 (2012) 98–106.
- 628 [16] I.I. Ozturk, A.K. Metsios, S. Filimonova-Orlova, N. Kourkoumelis, S.K. Hadjikakou, M.

- 629 Manos, A.J. Tasiopoulos, S. Karkabounas, E.R. Milaeva, N. Hadjiliadis, Study on single  
630 crystal structure of the antimony(III) bromide complex with  
631 3-methyl-2-mercaptobenzothiazole and biological activity of some antimony(III)  
632 bromide complexes with thioamides, *Med. Chem. Res.* 21 (2012) 3523–3531.
- 633 [17] O.S. Urgut, I.I. Ozturk, C.N. Banti, N. Kourkoumelis, M. Manoli, A.J. Tasiopoulos, S.K.  
634 Hadjikakou, New antimony (III) halide complexes with dithiocarbamate ligands derived  
635 from thiuram degradation: The effect of the molecule's close contacts on in vitro  
636 cytotoxic activity, *Mat. Sci. Eng. C-Mater.*, 58 (2016) 396–408.
- 637 [18] C. Silvestru, C. Socaciu, A. Bara, I. Haiduc, The first organoantimony(III) compounds  
638 possessing antitumor properties: diphenylantimony(III) derivatives of dithiophosphorus  
639 ligands, *Anticancer Res.* 10 (1990) 803–804.
- 640 [19] A. Bara, C. Socaciu, C. Silvestru, I. Haiduc, Antitumor organometallics. I. Activity of  
641 some diphenyltin(IV) and diphenylantimony(III) derivatives on in vitro and in vivo  
642 Ehrlich ascites tumor, *Anticancer Res.* 11 (1991) 1651–1655.
- 643 [20] C. Socaciu, A. Bara, C. Silvestru, I. Haiduc, Antitumor organometallics. II. Inhibitory  
644 effects of two diphenyl-antimony(III) dithiophosphorus derivatives on in vitro and in  
645 vivo Ehrlich ascites tumor. *In Vivo* 5 (1991) 425–428.
- 646 [21] B.K. Keppler, C. Silvestru, I. Haiduc, Antitumor organometallics. III. In vivo activity of  
647 diphenylantimony(III) and diorganotin(IV) dithiophosphorus derivatives against P388  
648 leukemia. *Metal-Based Drugs* 1 (1994) 73–77.
- 649 [22] C. Socaciu, I. Pasca, C. Silvestru, A. Bara, I. Haiduc, Antitumor organometallics. IV. The  
650 mutagenic potential of some diphenylantimony(III) dithiophosphorus derivatives.  
651 *Metal-Based Drugs* 1 (1994) 291–297.
- 652 [23] P. Naredi, D.D. Heath, R.E. Enns, S.B. Howell, Cross-resistance between cisplatin and  
653 antimony in a human ovarian carcinoma cell line. *Cancer Res.* 54 (1994) 6464–6468.
- 654 [24] P. Naredi, D.D. Heath, R. Enns, S.B. Howell, Cross-resistance between cisplatin,  
655 antimony potassium tartrate, and arsenite in human tumor cells, *J. Clin. Invest.* 95 (1995)  
656 1193-1198.
- 657 [25] C.E. Carraher Jr, M.D. Naas, D.J. Giron, D.R. Cerutis, Structural and biological  
658 characterization of antimony (V) polyamines, *J. Macromol. Sci. Chem.* 19 (1983) 1101–  
659 1120.
- 660 [26] L.G. de Oliveira, M.M. Silva, F.C.S. de Paula, E.C. Pereira-Maia, C.L. Donnici, C.A. de  
661 Simone, F. Frézard, E.N. da Silva Júnior, C. Demicheli, Antimony(V) and bismuth(V)  
662 complexes of lapachol: synthesis, crystal structure and cytotoxic activity, *Molecules* 16  
663 (2011) 10314–10323.
- 664 [27] A. Islam, B.L. Rodrigues, I.M. Marzano, E.C. Perreira-Maia, D. Dittz, L.M.T. Paz, M.  
665 Ishfaq, F. Frézard, C. Demicheli, Cytotoxicity and apoptotic activity of novel  
666 organobismuth(V) and organoantimony(V) complexes in different cancer cell lines, *Eur.*  
667 *J. Med. Chem.* 109 (2016) 254–267.
- 668 [28] J.-S. Li, Y.-Q. Ma, J.-R. Cui, R.-Q. Wang, Synthesis and in vitro antitumor activity of  
669 some tetraphenylantimony derivatives of exo-7-oxa-bicyclo[2,2,1] heptane  
670 (ene)-3-arylamide-2-acid, *Appl. Organomet. Chem.* 15 (2001) 639–645.
- 671 [29] G.C. Wang, J. Xiao, L. Yu, J.S. Li, J.R. Cui, R.Q. Wang, F.X. Ran, Synthesis, crystal  
672 structures and in vitro antitumor activities of some arylantimony derivatives of analogues

- 673 of demethylcantharimide. *J. Organomet. Chem.* 689 (2004) 1631–1638.
- 674 [30] Y. Chen, K. Yu, N.Y. Tan, R.H. Qiu, W. Liu, N.L. Luo, L. Tong, C.T. Au, Z.Q. Luo, S.F.  
675 Yin, Synthesis, characterization and anti-proliferative activity of heterocyclic hypervalent  
676 organoantimony compounds, *Eur. J. Med. Chem.* 79 (2014) 391–398.
- 677 [31] P. Pyykkö, M. Atsumi, Molecular single-bond covalent radii for elements 1–118,  
678 *Chem.-Eur. J.* 15 (2009) 186–197.
- 679 [32] S.S. Batsanov, Van der Waals Radii of elements, *Inorganic Materials* 37 (2001) 871–885.
- 680 [33] U. Ndagi, N. Mhlongo, M.E. Soliman, Metal complexes in cancer therapy—an update  
681 from drug design perspective. *Drug Des. Devel. Ther.* 11 (2017) 599–616.
- 682 [34] S. Dasari, P.B. Tchounwou, Cisplatin in cancer therapy: molecular mechanisms of action.  
683 *Eur. J. Pharmacol.* 740 (2014) 364–378.
- 684 [35] S. Elmore, Apoptosis: a review of programmed cell death. *Toxicol. Pathol.* 35 (2007)  
685 495–516.
- 686 [36] A. Hafner, M.L. Bulyk, A. Jambhekar, G. Lahav, The multiple mechanisms that regulate  
687 p53 activity and cell fate. *Nat. Rev. Mol. Cell Biol.* 2019.  
688 DOI:10.1038/s41580-019-0110-x.
- 689 [37] J.Z. Drago, S. Chandarlapaty, K. Jhaveri, Targeting Apoptosis: A New Paradigm for the  
690 Treatment of Estrogen Receptor-Positive Breast Cancer. *Cancer Discov.* 9 (2019) 323–  
691 325.
- 692 [38] F.K. Chan, K. Moriwaki, M.J. De Rosa, Detection of necrosis by release of lactate  
693 dehydrogenase activity. *Methods Mol. Biol.* 979 (2013) 65–70.
- 694 [39] B. Mery, J. Guy, A. Vallard, S. Espenel, D. Ardail, C. Rodriguez-Lafrasse, C. Rancoule,  
695 N. Magne, In vitro cell death determination for drug discovery: a landscape review of  
696 real issues. *J. Cell Death* 10 (2017) 1179670717691251.
- 697 [40] B.S. Cummings, R.G. Schnellmann, Measurement of cell death in mammalian cells. *Curr.*  
698 *Protoc. Pharmacol.* 1 (2004) 1–30.
- 699 [41] B. Zhou, J.Y. Zhang, X.S. Liu, H. Chen, Y. Ai, K. Cheng, R. Sun, D. Zhou, J. Han, Q.  
700 Wu, Tom20 senses iron-activated ROS signaling to promote melanoma cell pyroptosis.  
701 *Cell Res.* 28 (2018) 1171–1185.
- 702 [42] U. Ndagi, N. Mhlongo, M.E. Soliman, Metal complexes in cancer therapy—an update  
703 from drug design perspective. *Drug Des. Devel. Ther.* 11 (2017) 599–616.
- 704 [43] N. Kakusawa, Y. Tobiyasu, S. Yasuike, K. Yamaguchi, H. Seki, J. Kurita, Hypervalent  
705 organoantimony compounds 12-ethynyl-tetrahydrodibenz[*c,f*][1,5] azastibocines: highly  
706 efficient new transmetallating agent for organic halides, *J. Organomet. Chem.* 691 (2006)  
707 2953–2968.
- 708 [44] G.M. Sheldrick, SADABS, Empirical Absorption Correction Program, University of  
709 Gottingen, Germany, 1997.
- 710 [45] G.M. Sheldrick, A short history of SHELX, *Acta Crystallogr. A* 64 (2008) 112–122.
- 711 [46] Y.P. Liu, J. Lei, L.W. Tang, Y. Peng, C.T. Au, Y. Chen, S.F. Yin, Studies on the  
712 cytotoxicity and anticancer performance of heterocyclic hypervalent organobismuth (III)  
713 compounds. *Eur. J. Med. Chem.* 139 (2017) 826–835.

**Table 1**Selected bond lengths (Å) and angles (deg) of organoantimony(III) halide complexes **C1–C12**.

| <b>C1</b>        |           | <b>C2</b>        |           | <b>C3</b>       |           | <b>C4</b>        |           |
|------------------|-----------|------------------|-----------|-----------------|-----------|------------------|-----------|
| Sb(1)–C(1)       | 2.144(4)  | Sb(1)–C(6)       | 2.143(2)  | Sb(1)–C(6)      | 2.154(3)  | Sb(1)–C(6)       | 2.140(3)  |
| Sb(1)–C(8)       | 2.134(4)  | Sb(1)–C(10)      | 2.157(2)  | Sb(1)–C(7)      | 2.166(3)  | Sb(1)–C(7)       | 2.145(3)  |
| C(1)–Sb(1)–C(8)  | 98.2(1)   | C(6)–Sb(1)–C(10) | 99.23(8)  | C(6)–Sb(1)–C(7) | 98.8(1)   | C(6)–Sb(1)–C(7)  | 98.5(1)   |
| Cl(1)–Sb(1)–N(1) | 162.92(7) | Br(1)–Sb(1)–N(1) | 163.53(4) | I(1)–Sb(1)–N(1) | 163.34(6) | F(1)–Sb(1)–N(1)  | 156.42(7) |
| Sb(1)–N(1)       | 2.397(2)  | Sb(1)–N(1)       | 2.387(2)  | Sb(1)–N(1)      | 2.400(2)  | Sb(1)–N(1)       | 2.450(2)  |
| Sb(1)–Cl(1)      | 2.5572(9) | Sb(1)–Br(1)      | 2.7142(5) | Sb(1)–I(1)      | 2.9650(4) | Sb(1)–F(1)       | 2.015(2)  |
| <b>C5</b>        |           | <b>C6</b>        |           | <b>C7</b>       |           | <b>C8</b>        |           |
| Sb(1)–C(1)       | 2.150(2)  | Sb(1)–C(1)       | 2.158(3)  | Sb(1)–C(1)      | 2.166(3)  | Sb(1)–C(1)       | 2.131(3)  |
| Sb(1)–C(8)       | 2.155(2)  | Sb(1)–C(8)       | 2.156(3)  | Sb(1)–C(8)      | 2.175(3)  | Sb(1)–C(8)       | 2.153(3)  |
| C(1)–Sb(1)–C(8)  | 100.53(7) | C(1)–Sb(1)–C(8)  | 100.4(1)  | C(1)–Sb(1)–C(8) | 96.3(1)   | C(1)–Sb(1)–C(8)  | 91.80(9)  |
| Cl(1)–Sb(1)–N(1) | 161.98(4) | Br(1)–Sb(1)–N(1) | 163.22(6) | I(1)–Sb(1)–N(1) | 163.92(6) | F(1)–Sb(1)–N(1)  | 162.92(7) |
| Sb(1)–N(1)       | 2.466(2)  | Sb(1)–N(1)       | 2.469(2)  | Sb(1)–N(1)      | 2.498(3)  | Sb(1)–N(1)       | 2.522(2)  |
| Sb(1)–Cl(1)      | 2.5173(5) | Sb(1)–Br(1)      | 2.6620(4) | Sb(1)–I(1)      | 2.8995(3) | Sb(1)–F(1)       | 1.998(2)  |
| <b>C9</b>        |           | <b>C10</b>       |           | <b>C11</b>      |           | <b>C12</b>       |           |
| Sb(1)–C(1)       | 2.147(2)  | Sb(1)–C(6)       | 2.153(2)  | Sb(1)–C(6)      | 2.166(3)  | Sb(1)–C(6)       | 2.127(7)  |
| Sb(1)–C(14)      | 2.155(3)  | Sb(1)–C(7)       | 2.151(2)  | Sb(1)–C(7)      | 2.157(3)  | Sb(1)–C(10)      | 2.135(7)  |
| C(1)–Sb(1)–C(14) | 95.60(9)  | C(6)–Sb(1)–C(7)  | 96.18(8)  | C(6)–Sb(1)–C(7) | 97.6(1)   | C(6)–Sb(1)–C(10) | 98.2(3)   |
| Cl(1)–Sb(1)–N(1) | 161.60(5) | Br(1)–Sb(1)–N(1) | 162.99(4) | I(1)–Sb(1)–N(1) | 163.59(6) | F(1)–Sb(1)–N(1)  | 155.9(2)  |
| Sb(1)–N(1)       | 2.467(2)  | Sb(1)–N(1)       | 2.446(2)  | Sb(1)–N(1)      | 2.462(3)  | Sb(1)–N(1)       | 2.495(5)  |
| Sb(1)–Cl(1)      | 2.5579(7) | Sb(1)–Br(1)      | 2.7631(5) | Sb(1)–I(1)      | 2.9463(3) | Sb(1)–F(1)       | 2.026(6)  |

**Table 2**Crystallographic data for organoantimony(III) halide complexes **C1–C12**.

| Compound                             | <b>C1</b>                             | <b>C2</b>                             | <b>C3</b>                             | <b>C4</b>                             | <b>C5</b>                             | <b>C6</b>                             |
|--------------------------------------|---------------------------------------|---------------------------------------|---------------------------------------|---------------------------------------|---------------------------------------|---------------------------------------|
| Empirical formula                    | C <sub>20</sub> H <sub>23</sub> ClNSb | C <sub>20</sub> H <sub>23</sub> BrNSb | C <sub>20</sub> H <sub>23</sub> INSb  | C <sub>20</sub> H <sub>23</sub> FNSb  | C <sub>20</sub> H <sub>17</sub> ClNSb | C <sub>20</sub> H <sub>17</sub> BrNSb |
| Formula weight                       | 434.59                                | 479.05                                | 526.04                                | 418.14                                | 428.55                                | 473.01                                |
| Temperature/K                        | 293                                   | 273                                   | 100                                   | 100                                   | 273                                   | 298                                   |
| Crystal system                       | Monoclinic                            | monoclinic                            | monoclinic                            | monoclinic                            | Monoclinic                            | monoclinic                            |
| Space group                          | <i>P</i> <sub>2</sub> (1)/ <i>c</i>   | <i>P</i> <sub>2</sub> (1)/ <i>n</i>   |
| <i>a</i> /Å                          | 10.0771(7)                            | 10.2338(5)                            | 11.3664(3)                            | 9.3503(3)                             | 9.3782(4)                             | 9.5744(3)                             |
| <i>b</i> /Å                          | 16.2881(12)                           | 16.5885(7)                            | 12.5996(3)                            | 15.9263(5)                            | 10.1833(4)                            | 10.2962(3)                            |
| <i>c</i> /Å                          | 12.2040(9)                            | 12.0033(5)                            | 13.0792(4)                            | 11.7239(4)                            | 18.1033(8)                            | 18.1939(6)                            |
| $\alpha$ /°                          | 90.00                                 | 90.00                                 | 90.00                                 | 90.00                                 | 90.00                                 | 90.00                                 |
| $\beta$ /°                           | 111.812(10)                           | 113.346(2)                            | 94.703(2)                             | 104.044(3)                            | 102.895(10)                           | 100.795(1)                            |
| $\gamma$ /°                          | 90.00                                 | 90.00                                 | 90.00                                 | 90.00                                 | 90.00                                 | 90.00                                 |
| <i>V</i> /Å <sup>3</sup>             | 1859.7(2)                             | 1870.89(15)                           | 1866.79(9)                            | 1693.69(10)                           | 1685.3(12)                            | 1761.81(10)                           |
| <i>Z</i>                             | 4                                     | 4                                     | 4                                     | 4                                     | 4                                     | 4                                     |
| No. of reflections collected         | 10058                                 | 30234                                 | 12759                                 | 10827                                 | 9923                                  | 10613                                 |
| No. of unique reflections            | 3644                                  | 4636                                  | 3284                                  | 2982                                  | 4032                                  | 3417                                  |
| <i>R</i> <sub>int</sub>              | 0.047                                 | 0.0363                                | 0.0390                                | 0.0376                                | 0.015                                 | 0.038                                 |
| <i>R</i> <sub>1</sub> (reflections)  | 0.0324                                | 0.0196                                | 0.0236                                | 0.0256                                | 0.0203                                | 0.0294                                |
| <i>wR</i> <sub>2</sub> (reflections) | 0.0917                                | 0.0416                                | 0.0561                                | 0.0598                                | 0.0560                                | 0.0709                                |
| GOF on <i>F</i> <sup>2</sup>         | 1.048                                 | 1.066                                 | 1.022                                 | 1.097                                 | 1.077                                 | 1.041                                 |
| Compound                             | <b>C7</b>                             | <b>C8</b>                             | <b>C9</b>                             | <b>C10</b>                            | <b>C11</b>                            | <b>C12</b>                            |
| Empirical formula                    | C <sub>20</sub> H <sub>17</sub> INSb  | C <sub>20</sub> H <sub>17</sub> FNSb  | C <sub>18</sub> H <sub>21</sub> ClNSb | C <sub>18</sub> H <sub>21</sub> BrNSb | C <sub>18</sub> H <sub>21</sub> INSb  | C <sub>18</sub> H <sub>21</sub> FNSb  |
| Formula weight                       | 520.00                                | 412.10                                | 408.56                                | 453.02                                | 500.01                                | 392.11                                |
| Temperature/K                        | 298                                   | 293                                   | 273                                   | 273                                   | 100                                   | 273                                   |
| Crystal system                       | monoclinic                            | monoclinic                            | Monoclinic                            | monoclinic                            | monoclinic                            | monoclinic                            |
| Space group                          | <i>P</i> <sub>2</sub> (1)/ <i>c</i>   | <i>P</i> <sub>2</sub> (1)/ <i>n</i>   | <i>P</i> <sub>2</sub> (1)/ <i>n</i>   | <i>P</i> <sub>2</sub> (1)/ <i>n</i>   | <i>P</i> <sub>2</sub> (1)/ <i>c</i>   | <i>Cc</i>                             |
| <i>a</i> /Å                          | 9.1637(3)                             | 10.2974(8)                            | 9.7692(12)                            | 9.8178(4)                             | 12.3974(4)                            | 17.7432(9)                            |
| <i>b</i> /Å                          | 10.9833(4)                            | 10.3031(8)                            | 15.933(2)                             | 16.1278(5)                            | 9.4136(3)                             | 10.6409(6)                            |
| <i>c</i> /Å                          | 18.0957(7)                            | 15.7161(11)                           | 11.4491(14)                           | 11.4078(5)                            | 14.8803(5)                            | 17.8551(10)                           |
| $\alpha$ /°                          | 90.00                                 | 90.00                                 | 90.00                                 | 90.00                                 | 90.00                                 | 90.00                                 |
| $\beta$ /°                           | 95.784(1)                             | 101.559 (1)                           | 110.103(2)                            | 109.895(1)                            | 92.218(3)                             | 96.996(2)                             |
| $\gamma$ /°                          | 90.00                                 | 90.00                                 | 90.00                                 | 90.00                                 | 90.00                                 | 90.00                                 |
| <i>V</i> /Å <sup>3</sup>             | 1812.02(11)                           | 1633.6(2)                             | 1 673.5(4)                            | 1698.50(11)                           | 1735.29(10)                           | 3346.0(3)                             |
| <i>Z</i>                             | 4                                     | 4                                     | 4                                     | 4                                     | 4                                     | 8                                     |
| No. of reflections collected         | 9043                                  | 9422                                  | 9317                                  | 49645                                 | 11089                                 | 31989                                 |
| No. of unique reflections            | 3510                                  | 3560                                  | 3889                                  | 2978                                  | 3058                                  | 8232                                  |
| <i>R</i> <sub>int</sub>              | 0.055                                 | 0.063                                 | 0.027                                 | 0.0437                                | 0.0353                                | 0.0229                                |
| <i>R</i> <sub>1</sub> (reflections)  | 0.0354                                | 0.0323                                | 0.0326                                | 0.0143                                | 0.0237                                | 0.0419                                |
| <i>wR</i> <sub>2</sub> (reflections) | 0.0912                                | 0.0840                                | 0.0860                                | 0.0541                                | 0.0516                                | 0.1205                                |
| GOF on <i>F</i> <sup>2</sup>         | 1.070                                 | 1.065                                 | 1.058                                 | 1.028                                 | 1.040                                 | 1.079                                 |

**Table 3**

Cytotoxic effect of organoantimony(III) halide complexes **C1–C12**, nitrogen-containing precursors **P1–P3** and cisplatin on various cancerous and nonmalignant cell lines after 24 h

| Cell lines | HepG2                              |                 | MDA-MB-231            |                 | MCF-7                 |                 | HeLa                  |                 | HEK-293               |
|------------|------------------------------------|-----------------|-----------------------|-----------------|-----------------------|-----------------|-----------------------|-----------------|-----------------------|
| Compound   | IC <sub>50</sub> ± SD <sup>a</sup> | SI <sup>b</sup> | IC <sub>50</sub> ± SD | SI <sup>c</sup> | IC <sub>50</sub> ± SD | SI <sup>d</sup> | IC <sub>50</sub> ± SD | SI <sup>e</sup> | IC <sub>50</sub> ± SD |
| <b>C1</b>  | 1.84 ± 0.42                        | 5.05            | 1.40 ± 0.32           | 6.64            | 6.08 ± 1.38           | 1.53            | 1.63 ± 0.49           | 5.70            | 9.29 ± 1.16           |
| <b>C2</b>  | 4.86 ± 0.91                        | 2.10            | 3.63 ± 0.87           | 2.82            | 6.39 ± 1.45           | 1.60            | 3.12 ± 0.45           | 3.28            | 10.23 ± 0.55          |
| <b>C3</b>  | 1.61 ± 0.33                        | 5.63            | 1.28 ± 0.54           | 7.08            | 5.79 ± 1.56           | 1.56            | 1.13 ± 0.21           | 8.02            | 9.06 ± 1.31           |
| <b>C4</b>  | 1.06 ± 0.17                        | 7.15            | 0.91 ± 0.22           | 8.33            | 2.14 ± 0.93           | 3.54            | 0.93 ± 0.15           | 8.15            | 7.58 ± 0.89           |
| <b>C5</b>  | 2.78 ± 0.59                        | 3.07            | 1.72 ± 0.33           | 4.97            | 3.14 ± 0.81           | 2.72            | 3.32 ± 0.50           | 2.57            | 8.54 ± 1.88           |
| <b>C6</b>  | 1.90 ± 0.12                        | 4.10            | 1.05 ± 0.13           | 7.42            | 2.61 ± 0.60           | 2.98            | 2.34 ± 0.32           | 3.33            | 7.79 ± 1.36           |
| <b>C7</b>  | 1.87 ± 0.11                        | 3.33            | 1.04 ± 0.11           | 5.98            | 2.39 ± 1.67           | 2.60            | 2.06 ± 0.29           | 3.02            | 6.22 ± 1.69           |
| <b>C8</b>  | 0.88 ± 0.32                        | 4.41            | 0.52 ± 0.02           | 7.46            | 2.31 ± 0.32           | 1.68            | 1.12 ± 0.21           | 3.46            | 3.88 ± 1.01           |
| <b>C9</b>  | 1.41 ± 0.06                        | 4.03            | 0.84 ± 0.23           | 6.76            | 3.41 ± 0.30           | 1.67            | 1.98 ± 0.54           | 2.87            | 5.68 ± 1.32           |
| <b>C10</b> | 2.74 ± 0.63                        | 2.27            | 1.85 ± 0.25           | 3.36            | 6.34 ± 1.31           | 0.98            | 4.78 ± 0.83           | 1.30            | 6.22 ± 1.07           |
| <b>C11</b> | 1.84 ± 0.28                        | 4.05            | 0.97 ± 0.19           | 7.69            | 4.89 ± 1.13           | 1.53            | 2.09 ± 0.62           | 3.57            | 7.46 ± 0.66           |
| <b>C12</b> | 0.71 ± 0.06                        | 3.51            | 0.51 ± 0.12           | 4.88            | 0.96 ± 0.83           | 2.59            | 1.08 ± 0.47           | 2.31            | 2.49 ± 0.67           |
| <b>P1</b>  | > 50.00                            | –               | > 50.00               | –               | > 50.00               | –               | > 50.00               | –               | > 50.00               |
| <b>P2</b>  | > 50.00                            | –               | > 50.00               | –               | > 50.00               | –               | > 50.00               | –               | > 50.00               |
| <b>P3</b>  | > 50.00                            | –               | > 50.00               | –               | > 50.00               | –               | > 50.00               | –               | > 50.00               |
| cisplatin  | 13.19 ± 4.51                       | 3.71            | 12.63 ± 1.22          | 3.88            | 22.75 ± 8.59          | 2.15            | 17.35 ± 3.64          | 2.82            | 48.96 ± 8.75          |

Cancerous Cell Lines: HepG2 (human liver hepatocellular carcinoma cell line), MDA-MB-231 (human breast cancer cell line), MCF-7 (human breast adenocarcinoma cell line) and HeLa (human cervical carcinoma cell line). Nonmalignant Cell Line: HEK-293 (human embryonic kidney cell line). IC<sub>50</sub>: concentration that is cytotoxic against 50% of cell lines. SI: selectivity index. <sup>a</sup>The IC<sub>50</sub> values were determined through non-linear regression analysis; Each well was triplicated and each experiment was repeated at least three times. IC<sub>50</sub> values quoted are mean ± SD (μM). <sup>b</sup>Calculated as the ratio between IC<sub>50</sub> in HEK-293 cells and IC<sub>50</sub> in HepG2. <sup>c</sup>Calculated as the ratio between IC<sub>50</sub> in HEK-293 cells and IC<sub>50</sub> in MDA-MB-231. <sup>d</sup>Calculated as the ratio between IC<sub>50</sub> in HEK-293 cells and IC<sub>50</sub> in MCF-7. <sup>e</sup>Calculated as the ratio between IC<sub>50</sub> in HEK-293 cells and IC<sub>50</sub> in HeLa.

**Highlights**

- Cytotoxicity against human cancerous cell lines of Sb(III) halide complexes was evaluated.
- The cytotoxicity was closely related to the N→Sb coordinate bond length.
- Sb(III) complex **C4** exhibited the highest selectivity index.
- **C4** induced S phase cell cycle arrest and necrosis in MDA-MB-231 cells.
- The cytotoxicity was dependent on the production of intracellular reactive oxygen species.